Optimal Dynamic Asset Allocation for DC Plan Accumulation/Decumulation: Ambition-CVAR

Peter A. Forsyth[a]

April 20, 2020

Abstract

We consider the late accumulation stage, followed by the full decumulation stage, of an investor in a defined contribution (DC) pension plan. The investor's portfolio consists of a stock index and a bond index. As a measure of risk, we use conditional value at risk (CVAR) at the end of the decumulation stage. This is a measure of the risk of depleting the DC plan, which is primarily driven by sequence of return risk and asset allocation during the decumulation stage. As a measure of reward, we use Ambition, which we define to be the probability that the terminal wealth exceeds a specified level. We develop a method for computing the optimal dynamic asset allocation strategy which generates points on the efficient Ambition-CVAR frontier. By examining the Ambition-CVAR efficient frontier, we can determine points that are Median-CVAR optimal. We carry out numerical tests comparing the Median-CVAR optimal strategy to a benchmark constant proportion strategy. For a fixed median value (from the benchmark strategy) we find that the optimal Median-CVAR control significantly improves the CVAR. In addition, the median allocation to stocks at retirement is considerably smaller than the benchmark allocation to stocks.

Keywords: optimal control, ambition-CVAR, asset allocation, DC plan, resampled backtests
JEL codes: G11, G22
AMS codes: 91G, 65N06, 65N12, 35Q93

1 Introduction

In the pension benefit world, it is clear that the prevailing trend is towards the elimination of defined benefit (DB) plans, in favour of defined contribution (DC) plans.[1] This is simply a result of the desire of many corporations (and government institutions) to de-risk their balance sheets. In some countries, including Australia and the United States, the majority of pension fund assets are currently held in DC plans rather than DB plans.[2]

[a]David R. Cheriton School of Computer Science, University of Waterloo, Waterloo ON, Canada N2L 3G1, paforsyt@uwaterloo.ca, +1 519 888 4567 ext. 34415.

[1]See, for example, *"The extinction of defined-benefit plans is almost upon us,"* Globe and Mail, October 4, 2018. https://www.theglobeandmail.com/investing/personal-finance/retirement/article-the-extinction-of-defined-benefit-pension-plans-is-almost-upon-us/

[2]See the Thinking Ahead Institute's *"Global Pension Assets Study 2018"*, www.thinkingaheadinstitute.org/-/media/Pdf/TAI/Research-Ideas/GPAS-2018.pdf

A typical DC plan requires the employee and employer to contribute a fraction of the employee's yearly salary into a tax-advantaged retirement account, during the accumulation phase. The employee then determines how to invest the accumulated funds. Usually, there is a menu of choices available, primarily stock and bond index funds. Once the employee retires (the decumulation phase), the employee must select (i) a yearly withdrawal amount from the DC account and (ii) an asset allocation strategy. The risk faced by the retiree during the decumulation phase is that investment returns may be insufficient to fund the withdrawals, and the retiree may run out of savings.

Although it is commonplace in the academic literature to suggest that DC plan holders should purchase an annuity upon retirement, this rarely occurs in practice (Peijnenburg et al., 2016). MacDonald et al. (2013) list a variety of reasons why investors do not purchase annuities, such as poor pricing, lack of true inflation protection, no possible legacy, and no access to capital in the event of emergencies.

Target Date Funds (TDFs) (Basu et al., 2011) are popular products which have seen widespread adoption in recent years. *To and through* TDFs are suggested to be a possible method for handling asset allocation strategies for DC plan holders during accumulation and decumulation phases. These TDFs use deterministic, age dependent strategies, which typically have high equity weights during the early accumulation years, which decrease as the plan holder nears retirement. Some practitioners then advocate a gradual in increase in equity weights after retirement, to reduce the risk of exhausting savings (Kitces and Pfau, 2015). At the end of 2019, in the US, there was over $1.4 trillion of DC plan assets invested in TDFs.[3].

However, recent research has cast doubt on deterministic asset allocation strategies. Graf (2017); Forsyth and Vetzal (2019) find that deterministic strategies are no better than constant weight strategies with the constant weight selected as the time averaged deterministic equity weight. Empirical backtests support this conclusion (Poterba et al., 2009; Esch and Michaud, 2014).

Another possible method for generating guaranteed cash flows during retirement is a variable annuity. As pointed out in Horneff et al. (2015), variable annuities with guaranteed cash flows are specifically designed to mitigate decumulation risk. A typical example of this sort of contract is a Guaranteed Lifelong Withdrawal Benefit (GLWB) (Piscopo and Haberman, 2011; Forsyth and Vetzal, 2014; Feng and Yi, 2019). This contract allows more investor control over assets compared with a traditional annuity, and provides a guaranteed lifelong cash flow which has some inflation protection, due to ratchet type guarantees based on market performance. However, after the financial crisis, many insurance companies exited the variable annuity business, or reduced benefits and increased fees. Variable annuities are regarded as unattractive now by many financial advisors.[4]

A standard technique used in the literature for DC plan asset allocation involves the use of utility functions, see, for example Blake et al. (2014); Campanele et al. (2015); Michaelides and Zhang (2017). However, as noted by Vigna (2014), traditional utility functions used in the economic literature often have obscure parameters, which would be difficult to interpret for retail investors. Based on objective functions and asset allocation strategies which are easily explainable, Forsyth et al. (2019) compare strategies based on such criteria as minimizing probability of ruin and quadratic shortfall.

Another strand of literature is empirical, i.e. based on studying how people nearing retirement actually invest (Fagereng et al., 2017). There is, of course, no reason to suppose that current retail investors' strategies are optimal in any sense.

[3]`https://www.investmentnews.com/target-date-sales-returns-up-2019-187835`

[4]See, for example, *"5 Reasons Why You Should Never Buy A Variable Annuity,"* `https://www.forbes.com/sites/jrose/2015/03/28/5-reasons-why-you-should-never-buy-a-variable-annuity`

We should mention the recent literature on the use of modern tontines. Modern tontines (Milevsky and Salisbury, 2015; Braughtigam et al., 2017) allow investors to pool longevity risk without having to buy an annuity. There is, however, no guarantee of cash flows. Hence the expected return on a pure tontine is higher than that of an annuity.

There is a standard rule-of-thumb advocated by financial planners for decumulation strategies, which relies on the *4 per cent rule*. Based on historical backtests, Bengen (1994) suggests investing 50% in bonds and 50% in stocks, and rebalancing annually. The backtests, based on rolling 30 year periods, show that if the investor withdraws 4% of the initial value of the portfolio for 30 years (the withdrawals are escalated to preserve real purchasing power) and rebalances annually, then the investor would have never depleted their portfolio over any historical rolling 30 year period. Increasing the withdrawal rate significantly resulted in depletion of the portfolio during some historical periods.

A more recent spending rule strategy is based on an Annually Recalculated Virtual Annuity (ARVA). The ARVA strategy determines the yearly spending amount based on the current portfolio wealth, and the amount that would be generated by a virtual fixed term annuity, computed each year. Westmacott and Daley (2015) suggests using a fixed term, which is recomputed each year, based on outliving 80% of the retiree's peers. This ARVA rule takes into account mortality effects, and is guaranteed never to exhaust the portfolio. However, this comes at the cost of possibly highly variable withdrawal amounts each year (Waring and Siegel, 2015; Westmacott and Daley, 2015; Forsyth et al., 2020). In fact, the withdrawal amount may become very small.

For an extensive review of strategies during the decumulation phase, we refer the reader to (MacDonald et al., 2013). In addition, Bernhardt and Donnelly (2018) discuss a variety of concerns of DC plan investors, including bequest motives, the possibility of running out of savings, and maximizing real (inflation adjusted) withdrawals. The authors discuss the merits and demerits of the utility function approach, practitioner rules of thumb, target based approaches, minimizing the probability of ruin, and the use of tontines. The authors note that typical constant weight or glide path strategies often have non-negligible probabilities of both tail events, in which the investor runs out of savings, or ends up leaving a very large bequest. Neither of these outcomes is (presumably) desirable. The authors conclude

> *"There are many ways of solving the problem of how much to withdraw as income and how to invest savings in retirement. There is no solution that is appropriate for everyone and neither is there a single solution for any individual."* (Bernhardt and Donnelly, 2018)

A survey revealed the unexpected result that the majority of respondents feared outliving their assets more than dying.[5] In view of this fact, our objective in this paper is to focus on conservative asset allocation strategies which minimize worst case scenario risk. Of course, it must be recognized that investing solely in low-risk assets (e.g. bonds) will result in a high probability of portfolio depletion, with any reasonable withdrawal rate.

As a measure of risk, we will use the Conditional Value at Risk, denoted by CVAR_α, which is the mean of the worst α fraction of outcomes. Note that we have defined CVAR here in terms of terminal wealth, not losses. Hence a larger value of CVAR is desirable, i.e. has less risk. CVAR has the convenient intuitive interpretation as the dollar risk of depleting the DC plan account at the end of the decumulation stage. It is then possible for the DC plan holder to compare this risk with other possible assets (e.g. the retiree's home).

[5] *"Reclaiming the future,"* Allianz Life Insurance Company of North America, White paper, 2010

Note that a major problem with a DC plan is sequence of return risk during the decumulation stage. A sequence of poor returns, during the initial decumulation stage, has a devastating impact on the portfolio at later times. Although a sequence of poor returns immediately after retirement is a fairly low probability event, this will lead to early depletion of the retirement account. Consequently, we consider the CVAR of the terminal wealth as an appropriate measure of the consequences of sequence of return risk.

Let W_T be the terminal wealth at time T. As a measure of reward, we will use Ambition A_β, which we define to be $Pr[W_T > \beta]$. Using this definition of reward will ensure that rare events with large payoffs will not skew the results, consistent with our search for a conservative strategy. The multi-period Pareto optimal Ambition-CVAR strategies will form an Ambition-CVAR efficient frontier. The point on this frontier where $A_\beta = .50$ is Median-CVAR optimal, in the sense that with this fixed value of median β, no other strategy has a larger (more desirable) CVAR.

We remark that the CVAR above is determined at the initial time, with the consequence that this is a pre-commitment strategy. However, this strategy (at time zero) is identical to the optimal control for an induced time consistent objective function, hence is implementable. This is discussed at some length in Forsyth (2020). The concept of an induced time consistent strategy is also addressed in Strub et al. (2019).

We first devise a method to compute points on the Ambition-CVAR efficient frontier. Then, given a benchmark strategy with generates a given median terminal wealth $Median[W_T]$, we search for the point on the Ambition-CVAR efficient frontier, which has the same $Median[W_T]$. This gives us the strategy which generates the largest possible CVAR, for this $Median[W_T]$.

In our numerical examples, we consider a two asset portfolio, consisting of a stock index and a constant maturity bond index. We consider an investor in the late accumulation stage, followed by the full decumulation stage. Consequently, this example will focus on the effects of sequence of return risk during the decumulation stage.

We fit the stochastic process parameters to historical monthly real (i.e. inflation adjusted) return data in the range *1926:1-2018:12*. We term the market where the assets follow the parametric model fit to the long term data the *synthetic market*. For our benchmark strategy, we consider a constant proportion policy, where rebalancing is carried out annually, in the synthetic market. We then determine (numerically) points which are Median-CVAR optimal, so that $Median[W_T]$ is the same as given from the benchmark strategy.

We examine two cases for the benchmark policy: a conservative investor and an aggressive investor. In both cases, the Median-CVAR optimal strategy has the same $Median[W_T]$ as the benchmark strategy, but significantly improved CVAR_α.

We compute and store optimal dynamic Median-CVAR controls in the synthetic market. Then, we use these controls in bootstrapped resampling tests based on historical market returns. In this *historical market*, we see once again that the Median-CVAR optimal control produces essentially the same $Median[W_t]$ as the benchmark constant proportion strategy, but with much improved CVAR_α. This indicates that our conclusions are robust to parametric model misspecification.

It is interesting to observe from the control heat maps for the Median-CVAR optimal strategy, that the regions of high bond weightings (as a function of wealth and time) are multiply connected. This is due to the objective function, which puts a high priority on protecting the CVAR_α. Only after we have a high probability of achieving the specified value of CVAR_α does the strategy switch to attempting to hit the $Median[W_T]$ target. This is very unusual type of control, and contrasts to the controls observed in Forsyth et al. (2019), where the high bond control regions are singly connected.

In summary, the choice of a dynamic Median-CVAR optimal strategy demonstrably outperforms a constant proportion strategy (in terms of median and CVAR). This result holds in both the synthetic market and a bootstrapped historical market. In addition, the median allocation to stocks at retirement, for the Median-CVAR optimal strategy is considerably smaller than the constant proportion benchmark policy. This is a desirable characteristic for a DC plan strategy.

However, directly targeting tail risk (as measured by CVAR) comes at a cost.

- It is relatively expensive to reduce risk, in the sense that small improvements in CVAR are costly in terms of reduced Median values of terminal wealth.
- The optimal Median-CVAR strategy is a complex function of wealth and time-to-go.

These results show that it is difficult to reduce the tail-risk in the decumulation stage of a DC plan, even using an optimal strategy. This suggests that there is a need for a financial product (available at reasonable cost) to mitigate this remaining risk.

2 Formulation

We assume that the investor has access to two funds: a broad market stock index fund and a constant maturity bond index fund.

The investment horizon is T. Let S_t and B_t respectively denote the real (inflation adjusted) *amounts* invested in the stock index and the bond index respectively. In general, these amounts will depend on the investor's strategy over time, as well as changes in the real unit prices of the assets. In the absence of an investor determined control (i.e. cash injections or rebalancing), all changes in S_t and B_t result from changes in asset prices. We model the stock index as following a jump diffusion.

In addition, we follow the usual practitioner approach and directly model the returns of the constant maturity bond index as a stochastic process, see for example Lin et al. (2015); MacMinn et al. (2014). This avoids the intermediate step of postulating a real interest rate process, and has the advantage that estimating model parameters is straightforward. As in MacMinn et al. (2014), we assume that the constant maturity bond index follows a jump diffusion process as well.

Let $S_{t^-} = S(t-\epsilon), \epsilon \to 0^+$, i.e. t^- is the instant of time before t, and let ξ^s be a random number representing a jump multiplier. When a jump occurs, $S_t = \xi^s S_{t^-}$. Allowing for jumps permits modelling of non-normal asset returns. We assume that $\log(\xi^s)$ follows a double exponential distribution (Kou, 2002; Kou and Wang, 2004). If a jump occurs, p_u^s is the probability of an upward jump, while $1 - p_u^s$ is the chance of a downward jump. The density function for $y = \log(\xi^s)$ is

$$f^s(y) = p_u^s \eta_1^s e^{-\eta_1^s y} \mathbf{1}_{y \geq 0} + (1 - p_u^s) \eta_2^s e^{\eta_2^s y} \mathbf{1}_{y < 0} , \tag{2.1}$$

where $1/\eta_1^s$ is the mean upward jump size, and $1/\eta_2^s$ is the mean downward jump size. We also define

$$\zeta^s = E[\xi^s - 1] = \frac{p_u^s \eta_1^s}{\eta_1^s - 1} + \frac{(1 - p_u^s)\eta_2^s}{\eta_2^s + 1} - 1 . \tag{2.2}$$

In the absence of control, S_t evolves according to

$$\frac{dS_t}{S_{t^-}} = \left(\mu^s - \lambda_\xi^s \zeta^s\right) dt + \sigma^s \, dZ^s + d\left(\sum_{i=1}^{\pi_t^s} (\xi_i^s - 1)\right) , \tag{2.3}$$

where μ^s is the (uncompensated) drift rate, σ^s is the volatility, dZ^s is the increment of a Wiener process, π_t^s is a Poisson process with positive intensity parameter λ_ξ^s, and ξ_i^s are i.i.d. positive random variables having distribution (2.1). Moreover, ξ_i^s, π_t^s, and Z^s are assumed to all be mutually independent.

Similarly, let the amount in bonds be $B_{t^-} = B(t-\epsilon), \epsilon \to 0^+$. In the absence of control, B_t evolves as

$$\frac{dB_t}{B_{t^-}} = \left(\mu^b - \lambda_\xi^b \zeta^b + \mu_c^b \mathbf{1}_{\{B_{t^-}<0\}}\right) dt + \sigma^b \, dZ^b + d\left(\sum_{i=1}^{\pi_t^b} (\xi_i^b - 1)\right), \tag{2.4}$$

where the terms in equation (2.4) are defined analogously to equation (2.3). In particular, π_t^b is a Poisson process with positive intensity parameter λ_ξ^b, and ξ_i^b has distribution

$$f^b(y = \log \xi^b) = p_u^b \eta_1^b e^{-\eta_1^b y} \mathbf{1}_{y \geq 0} + (1 - p_u^b) \eta_2^b e^{\eta_2^b y} \mathbf{1}_{y<0} \ , \tag{2.5}$$

and $\zeta^b = E[\xi^b - 1]$. ξ_i^b, π_t^b, and Z^b are assumed to all be mutually independent. The term $\mu_c^b \mathbf{1}_{\{B_{t^-}<0\}}$ in equation (2.4) represents the extra cost of borrowing (the spread).

The diffusion processes are correlated, i.e. $dZ^s \cdot dZ^b = \rho_{sb} dt$. The stock and bond jump processes are assumed mutually independent.

Remark 2.1 (Stock and Bond Processes)**.** *Equations (2.3) and (2.4) can be enhanced in many ways, such as including stochastic volatility effects. However, previous studies have shown that stochastic volatility appears to have little consequences for long term investors (Ma and Forsyth, 2016).*

Note that we have also assumed that the stock and bond jump processes are independent, see Appendix A for an analysis of the historical data which suggests that this is a reasonable approximation. At the other extreme, it is possible to assume that the jump processes are described by a common-shock structure (Xu, 2018). More generally, the jump process could be modelled using a full two factor jump process with general distributions (Clift and Forsyth, 2008), and all the methods described in this paper could be used in this case as well.

As a robustness check, we will (i) determine the optimal controls using the parametric model based on equations (2.3) and (2.4) and (ii) use these controls on bootstrapped resampled historical data, which makes no assumptions about the underlying bond and stock stochastic processes.

We define the investor's total wealth at time t as

$$\text{Total wealth } \equiv W_t = S_t + B_t. \tag{2.6}$$

We impose the constraints that (assuming solvency) shorting stock and using leverage (i.e. borrowing) are not permitted, which would be typical of a DC plan retirement savings account. In the event of insolvency (due to withdrawals), the portfolio is liquidated, trading ceases and debt accumulates at the borrowing rate.

3 Notational Conventions

To avoid subscript clutter, in the following, we will occasionally use the notation $S_t \equiv S(t), B_t \equiv B(t)$ and $W_t \equiv W(t)$. Let the inception time of the investment be $t_0 = 0$. We consider a set $\mathcal{T}$ of pre-determined *rebalancing times*,

$$\mathcal{T} \equiv \{t_0 = 0 < t_1 < \cdots < t_M = T\}. \tag{3.1}$$

For simplicity, we specify $\mathcal{T}$ to be equidistant with $t_i - t_{i-1} = \Delta t = T/M$, $i = 1, \ldots, M$. At each rebalancing time t_i, $i = 0, 1, \ldots, M-1$, the investor (i) injects an amount of cash q_i into the portfolio, and then (ii) rebalances the portfolio. At $t_M = T$, the final cash flow q_M occurs, and the portfolio is liquidated. Note that cash flows can be positive (injection) or negative (withdrawals). In the following, given a time dependent function $f(t)$, then we will use the shorthand notation

$$f(t_i^+) \equiv \lim_{\epsilon \to 0^+} f(t_i + \epsilon) \quad ; \quad f(t_i^-) \equiv \lim_{\epsilon \to 0^+} f(t_i - \epsilon) \ . \tag{3.2}$$

We assume that there are no taxes or other transaction costs, so that the condition

$$W(t_i^+) = W(t_i^-) + q_i \ , \tag{3.3}$$

holds. Typically, DC plan savings are held in a tax advantaged account, with no taxes triggered by rebalancing. With infrequent (e.g. yearly) rebalancing, we also expect transaction costs to be small, and hence can be ignored. It is possible to include transaction costs, but at the expense of increased computational cost (Staden et al., 2018).

We denote by $X(t) = (S(t), B(t))$, $t \in [0,T]$, the multi-dimensional controlled underlying process, and by $x = (s, b)$ the realized state of the system.

Let the rebalancing control $p_i(\cdot)$ be the fraction invested in the stock index at the rebalancing date t_i, after cash injection. Generally, $p_i(\cdot)$ would be a function of all the state variables at t_i^-. However, since we search for the optimal strategy amongst all strategies with constant wealth, after cash flows, then

$$\begin{aligned} p_i(\cdot) &= p(S(t_i^-) + B(t_i^-) + q_i, t_i) = p(W(t_i^+), t_i) \\ & \quad W(t_i^+) = S(t_i^-) + B(t_i^-) + q_i \\ & \quad S(t_i^+) = S_i^+ = p_i(W_i^+)\ W_i^+ \ ; \ B(t_i^+) = B_i^+ = (1 - p_i(W_i^+))\ W_i^+ \ . \end{aligned} \tag{3.4}$$

Remark 3.1 (Functions of stochastic process or state.)**.** *In the following, we will regard the control $p_i(\cdot)$ to be a function of the stochastic process variables, i.e. $p_i(\cdot) = p(S(t_i^-) + B(t_i^-) + q_i, t_i)$ or the state variables $p_i(\cdot) = p(s + b + q_i, t_i)$ depending on the context.*

Let $\mathcal{Z}$ represent the set of admissible values of the control $p_i(\cdot)$. An admissible control $\mathcal{P} \in \mathcal{A}$, where $\mathcal{A}$ is the admissible control set, can be written as

$$\mathcal{P} = \{p_i(\cdot) \in \mathcal{Z} \ : \ i = 0, \ldots, M-1\} \ . \tag{3.5}$$

As is typical for a DC plan savings account, we impose no-shorting, no-leverage constraints

$$\mathcal{Z} = [0,1] \ . \tag{3.6}$$

We also apply the constraint that in the event of insolvency ($W(t_i^+) < 0$), trading ceases and debt (negative wealth) accumulates at the appropriate bond rate of return (including a spread), i.e.

$$p(W(t_i^+), t_i) \quad = \quad 0 \ ; \quad \text{if } W(t_i^+) < 0 \ . \tag{3.7}$$

We also define $\mathcal{P}_n \equiv \mathcal{P}_{t_n} \subset \mathcal{P}$ as the tail of the set of controls in $[t_n, t_{n+1}, \ldots, t_{M-1}]$, i.e.

$$\mathcal{P}_n = \{p_n(\cdot), \ldots, p_{M-1}(\cdot)\} \ . \tag{3.8}$$

4 A Measure of Risk: Definition of CVAR

Let $g(W_T)$ be the probability density function of wealth W_T at $t = T$. Let

$$\int_{-\infty}^{W_\alpha^*} g(W_T)\ dW_T = \alpha, \tag{4.1}$$

i.e. $Pr[W_T > W_\alpha^*] = 1 - \alpha$. We can interpret W_α^* as the Value at Risk (VAR) at level α. The Conditional Value at Risk (CVAR) at level α is then

$$\text{CVAR}_\alpha = \frac{\int_{-\infty}^{W_\alpha^*} W_T\ g(W_T)\ dW_T}{\alpha}, \tag{4.2}$$

which is the mean of the worst α fraction of outcomes. Typically $\alpha \in \{.01, .05\}$. Note that the definition of CVAR in equation (4.2) uses the probability density of the final wealth distribution, not the density of *loss*. Hence, in our case, a larger value of CVAR (i.e. a larger value of average worst case terminal wealth) is desired.

Define $X_0^+ = X(t_0^+), X_0^- = X(t_0^-)$. Given an expectation under control $\mathcal{P}$, $E_{\mathcal{P}}[\cdot]$, as noted by Rockafellar and Uryasev (2000), CVAR_α can be alternatively written as

$$\text{CVAR}_\alpha(X_0^-, t_0^-) \quad = \quad \sup_{W^*} E_{\mathcal{P}_0}^{X_0^+, t_0^+}\left[W^* + \frac{1}{\alpha} \min(W_T - W^*, 0) \right]. \tag{4.3}$$

The admissible set for W^* in equation (4.3) is over the set of possible values for W_T.

Note that the notation $\text{CVAR}_\alpha(X_0^-, t_0^-)$ emphasizes that CVAR_α is as seen at (X_0^-, t_0^-). In other words, this is the pre-commitment CVAR_α. A strategy based purely on optimizing the pre-commitment value of CVAR_α at time zero is *time-inconsistent*, hence has been termed by many as *non-implementable*, since the investor has an incentive to deviate from the the pre-commitment strategy at $t > 0$. However, in the following, we will consider the pre-commitment strategy merely as a device to determine an appropriate level of W^* in equation (4.3). If we fix W^* $\forall t > 0$, then this strategy is the induced time consistent strategy (Strub et al., 2019), hence is implementable. We delay further discussion of this subtle point to later sections.

4.1 Bounds on CVAR

From equation (4.2)

$$\begin{aligned} \left| \frac{1}{\alpha} \int_{-\infty}^{W_\alpha^*} W_T\ g(W_T)\ dW_T \right| &= \frac{1}{\alpha} \left| \int_{-\infty}^{\min(W_\alpha^*, 0)} W_T\ g(W_T)\ dW_T + \int_{0}^{\max(W_\alpha^*, 0)} W_T\ g(W_T)\ dW_T \right| \\ &\leq \frac{1}{\alpha} \left| \int_{-\infty}^{0} W_T\ g(W_T)\ dW_T \right| + \frac{1}{\alpha} \left| \int_{0}^{\infty} W_T\ g(W_T)\ dW_T \right|. \end{aligned} \tag{4.4}$$

Define

$$Q^+ = \sum_{i=0}^{i=M} \max(q_i, 0) + W_0 \quad ; \quad Q^- = \sum_{i=0}^{i=M} \min(q_i, 0)\ , \tag{4.5}$$

where $W_0 = S_0 + B_0 \geq 0$. Note that due to the form of the SDEs (2.3) and (2.4), and the no-shorting, no-leverage constraint (3.6), then $W_T < 0$ can only be a result of withdrawals. Once insolvency occurs (i.e. $W_t < 0$), then trading ceases as in equation (3.7). Trading can resume only if future cash injections restore solvency. Assuming that $\mu^s > \mu^b$ (which would normally be the case), then the maximum expected value of terminal wealth occurs in the case of an all-stock portfolio. These facts allow us to determine the following bounds:

$$\begin{aligned} \left| \int_{-\infty}^{0} W_T \ g(W_T) \ dW_T \right| &\leq |Q^-| e^{(\mu^b + \mu_c^b)T} \\ \left| \int_{0}^{\infty} W_T \ g(W_T) \ dW_T \right| &\leq Q^+ e^{\mu^s T} \ . \end{aligned} \tag{4.6}$$

Putting together equations (4.4)-(4.6) give us the following result

Proposition 4.1 (CVAR bound)**.** *Assuming that the stock and bond processes are given by equations (2.3) and (2.3), with no-shorting and no-leverage constraint (3.6), no trading if insolvent (3.7), and that $\mu^s > \mu^b$, we have that*

$$\left| CVAR_\alpha(X_0^-, t_0^-) \right| \leq \frac{1}{\alpha} |Q^-| e^{(\mu^b + \mu_c^b)T} + \frac{1}{\alpha} Q^+ e^{\mu^s T} = C_{\max} \ . \tag{4.7}$$

5 A Measure of Reward: Ambition

CVAR_α is a weighted measure of risk. A standard measure of reward is the expected value of final wealth, i.e. $E_{\mathcal{P}}[W_T]$. However, the expected value can be criticized as being too optimistic, since it overweights low-probability, large payout events. To avoid this, we define the Ambition measure of reward at level β, A_β as

$$A_\beta = E_{\mathcal{P}}[\mathbf{1}_{W_T > \beta}] \ , \tag{5.1}$$

which we recognize as $Pr[W_T > \beta]$.

6 Pareto Optimal Points

Recall that $X(t)$ denotes the multi-dimensional underlying controlled stochastic process, and x is the realized state of the stochastic system. $\mathcal{P}$ denotes the control, representing the strategy as function of the current state, i.e. $\mathcal{P}(\cdot) : (X(t),t) \mapsto \mathcal{P} = \mathcal{P}(X(t),t)$.

We introduce some definitions.

Definition 6.1. *Fix a control $\mathcal{P}(\cdot)$, CVAR parameter α, and Ambition level β, and let $(x_0, 0) \equiv (X(t = 0^-), t = 0^-)$ denote the initial state, and define*

$$\begin{aligned} CVAR_{\mathcal{P}(\cdot)}^{x_0,0} &= \sup_{W^*} \left\{ E_{\mathcal{P}_0}^{X_0^+,t_0^+} \left[W^* + \frac{1}{\alpha} \min(W_T - W^*,0) \middle| X(t_0^-) = x_0 \right] \right\} , \\ A_{\mathcal{P}(\cdot)}^{x_0,0} &= E_{\mathcal{P}_0}^{X_0^+,t_0^+} [\mathbf{1}_{W_T > \beta} | X(t_0^-) = x_0] \ . \end{aligned} \tag{6.1}$$

Now, consider all admissible controls $\mathcal{P}$ and let

$$\mathcal{Y}_{(\alpha,\beta)} = \left\{ \left(A_{\mathcal{P}(\cdot)}^{x_0,0} \ , \ CVAR_{\mathcal{P}(\cdot)}^{x_0,0} \right) : \mathcal{P}(\cdot) \ admissible \right\} , \tag{6.2}$$

denote the **achievable Ambition-CVAR objective set***, and $\overline{\mathcal{Y}}_{(\alpha,\beta)}$ denote its closure.*

Definition 6.2. *A point* $(\mathbb{A}_*, \mathbb{C}_*) \in \bar{\mathcal{Y}}_{(\alpha,\beta)}$ *is a* **Pareto (optimal) point** *if there exists no admissible strategy* $\mathcal{P}(\cdot)$ *such that*

$$\begin{aligned} &A^{x_0,0}_{\mathcal{P}(\cdot)} \geq \mathbb{A}_* \\ &CVAR^{x_0,0}_{\mathcal{P}(\cdot)} \geq \mathbb{C}_* \ , \end{aligned}$$

and at least one of the inequalities in equation (6.3) is strict. We denote by $\mathbb{P}$ *the set of Pareto (optimal) points. Note that* $\mathbb{P} \subseteq \bar{\mathcal{Y}}_{(\alpha,\beta)}$.

We can determine points in $\mathbb{P}$ using a standard scalarization method. For arbitrary scalar $\kappa > 0$, we define $\mathcal{S}_\kappa(\mathcal{Y}_{(\alpha,\beta)})$ to be the set of scalarization optimal points for the parameter κ

$$\mathcal{S}_\kappa(\mathcal{Y}_{(\alpha,\beta)}) \quad = \quad \{(\mathbb{A}_*, \mathbb{C}_*) \in \bar{\mathcal{Y}}_{(\alpha,\beta)} : \mathbb{C}_* + \kappa\mathbb{A}_* = \sup_{(\mathbb{A},\mathbb{C}) \in \mathcal{Y}_{(\alpha,\beta)}} (\mathbb{C} + \kappa\mathbb{A})\} \ . \tag{6.3}$$

Remark 6.1 (Economic meaning of κ.)**.** *Mathematically, the scalar* κ *is simply a device to convert a multi-objective optimization problem into a single objective function. However,* $1/\kappa$ *has the convenient interpretation as the investor's aversion to CVAR risk. If* $\kappa \to \infty$*, then the investor only desires to maximize* $Pr[W_T > \beta]$*. On the other hand, if* $\kappa \to 0$*, the the investor desires to maximize CVAR above all else.*

We then define the **Ambition-CVAR scalarization optimal set**, denoted by $\mathcal{S}(\mathcal{Y}_{(\alpha,\beta)})$, as

$$\mathcal{S}(\mathcal{Y}_{(\alpha,\beta)}) = \bigcup_{\kappa > 0} \mathcal{S}_\kappa(\mathcal{Y}_{(\alpha,\beta)}) \ , \tag{6.4}$$

where we note that it is possible for $\mathcal{S}_\kappa(\mathcal{Y}_{(\alpha,\beta)})$ to be empty for some $\kappa > 0$.

We recognize the difference between the set of all Ambition-CVAR Pareto optimal points $\mathbb{P}$ and the set of Ambition-CVAR scalarization optimal points $\mathcal{S}(\mathcal{Y}_{(\alpha,\beta)})$ defined in equation (6.4). In general, $\mathcal{S}(\mathcal{Y}_{(\alpha,\beta)}) \subseteq \mathbb{P}$. However, the converse may not hold, if the achievable Ambition-CVAR objective set $\mathcal{Y}_{(\alpha,\beta)}$ is not convex We restrict our attention to determining $\mathcal{S}(\mathcal{Y}_{(\alpha,\beta)})$.

Definition 6.3 (Supporting Hyperplane)**.** *A supporting hyperplane w.r.t.* $\mathcal{Y}_{(\alpha,\beta)}$ *exists at* $(\mathbb{A}_0, \mathbb{C}_0) \in \bar{\mathcal{Y}}_{(\alpha,\beta)}$ *if there exists* $\kappa \geq 0$ *such that,* $\forall (\mathbb{A}, \mathbb{C}) \in \mathcal{Y}_{(\alpha,\beta)}$

$$\mathbb{C} + \kappa\mathbb{A} \quad \leq \quad \mathbb{C}_0 + \kappa\mathbb{A}_0 \ . \tag{6.5}$$

An alternative geometric characterization of $\mathcal{S}(\mathcal{Y}_{(\alpha,\beta)})$ is the following, which follows immediately from Definition 6.3 and equation (6.3)

Proposition 6.1. *A point* $(\mathbb{A}_0, \mathbb{C}_0) \in \bar{\mathcal{Y}}_{(\alpha,\beta)}$ *is a point in* $\mathcal{S}(\mathcal{Y}_{(\alpha,\beta)})$ *if and only if* $(\mathbb{A}_0, \mathbb{C}_0)$ *has a supporting hyperplane w.r.t.* $\mathcal{Y}_{(\alpha,\beta)}$.

Lemma 6.1 (Nonemptyness)**.** *Assuming the conditions for Proposition 4.1 are satisfied, then* $\mathcal{S}_\kappa(\mathcal{Y}_{(\alpha,\beta)})$ *is nonempty* $\forall \kappa > 0$*, i.e.* $\exists (\mathbb{A}_0, \mathbb{C}_0) \in \bar{\mathcal{Y}}_{(\alpha,\beta)}$ *such that*

$$\mathbb{C}_0 + \kappa\mathbb{A}_0 \quad = \quad \sup_{(\mathbb{A},\mathbb{C}) \in \mathcal{Y}_{(\alpha,\beta)}} (\mathbb{C} + \kappa\mathbb{A}) \ . \tag{6.6}$$

Proof. Since $\kappa > 0$, $0 \leq \mathbb{A} \leq 1$, and $\mathbb{C} \leq C_{\max}$ from Proposition 4.1, then the objective function $\mathbb{C} + \kappa\mathbb{A}$ is bounded from above. □

Lemma 6.2 (Monotonicity properties). *Let* $(\mathbb{A}(\kappa), \mathbb{C}(\kappa)) \in \mathcal{S}_\kappa(\mathcal{Y}_{(\alpha,\beta)})$*, and* $(\mathbb{A}(\kappa'), \mathbb{C}(\kappa')) \in \mathcal{S}_{\kappa'}(\mathcal{Y}_{(\alpha,\beta)})$*. Then if* $\kappa' > \kappa$

$$\mathbb{A}(\kappa') \geq \mathbb{A}(\kappa) \quad \mathit{and} \quad \mathbb{C}(\kappa') \leq \mathbb{C}(\kappa) \ . \tag{6.7}$$

Proof. This proof is similar to that used in Dang et al. (2016). We include this for the reader's convenience. Choose $\kappa' > \kappa$. From Lemma 6.1, $\mathcal{S}_\kappa(\mathcal{Y}_{(\alpha,\beta)})$ and $\mathcal{S}_{\kappa'}(\mathcal{Y}_{(\alpha,\beta)})$ are non-empty. By definition

$$\mathbb{C}(\kappa) + \kappa\mathbb{A}(\kappa) \quad \geq \mathbb{C}(\kappa') + \kappa\mathbb{A}(\kappa') \tag{6.8}$$

$$\mathbb{C}(\kappa') + \kappa'\mathbb{A}(\kappa') \quad \geq \mathbb{C}(\kappa) + \kappa'\mathbb{A}(\kappa) \ . \tag{6.9}$$

From equation (6.9)

$$-(\mathbb{C}(\kappa) + \kappa'\mathbb{A}(\kappa)) \quad \geq \quad -(\mathbb{C}(\kappa') + \kappa'\mathbb{A}(\kappa')) \ . \tag{6.10}$$

Adding equations (6.8) and (6.10) gives

$$(\kappa - \kappa')(\mathbb{A}(\kappa)) - \mathbb{A}(\kappa')) \geq 0 \ , \tag{6.11}$$

which, noting that $(\kappa - \kappa') < 0$, gives

$$\mathbb{A}(\kappa') \geq \mathbb{A}(\kappa) \ . \tag{6.12}$$

Multiply equation (6.8) by κ' and equation (6.10) by κ gives

$$\kappa'\mathbb{C}(\kappa) + \kappa'\kappa\mathbb{A}(\kappa) \quad \geq \quad \kappa'\mathbb{C}(\kappa') + \kappa'\kappa\mathbb{A}(\kappa') \ , \tag{6.13}$$

$$-(\kappa\mathbb{C}(\kappa) + \kappa\kappa'\mathbb{A}(\kappa)) \quad \geq \quad -(\kappa\mathbb{C}(\kappa') + \kappa\kappa'\mathbb{A}(\kappa')) \ . \tag{6.14}$$

Adding equations (6.13) and (6.14) gives

$$(\kappa' - \kappa)\mathbb{C}(\kappa) \quad \geq \quad (\kappa' - \kappa)\mathbb{C}(\kappa') \ . \tag{6.15}$$

Noting that $(\kappa' - \kappa) > 0$, then equation (6.15) implies

$$\mathbb{C}(\kappa') \quad \leq \quad \mathbb{C}(\kappa) \ . \tag{6.16}$$

$\square$

6.1 Outperforming a benchmark strategy

Consider an arbitrary admissible benchmark strategy with control $\mathcal{P}^* \in \mathcal{A}$, with initial state X_0^-. This strategy generates $\text{CVAR}_{\mathcal{P}^*(\cdot)}^{x_0,0}$. Now, choose β^* such that

$$\text{A}_{\mathcal{P}^*(\cdot)}^{x_0,0} \quad = \quad E_{\mathcal{P}_0^*}^{X_0^+, t_0^+}[\mathbf{1}_{W_T > \beta^*}] = 0.5 \ , \tag{6.17}$$

so that β^* is the median under the strategy $\mathcal{P}^*$. Our objective is to determine a strategy which outperforms the benchmark strategy in the Pareto optimal sense.

Definition 6.4 (Outperformance)**.** *Given a benchmark strategy $\mathcal{P}^*$ which generates $(\widehat{\mathbb{A}}, \widehat{\mathbb{C}})$ such that*

$$(\widehat{\mathbb{A}}, \widehat{\mathbb{C}}) \;=\; \left(A^{x_0,0}_{\mathcal{P}^*(\cdot)} = 0.5, \, CVAR^{x_0,0}_{\mathcal{P}^*(\cdot)} \right) \in \overline{\mathcal{Y}}_{(\alpha,\beta^*)} \ , \tag{6.18}$$

then a strategy $\mathcal{P}(\cdot)$ which generates $(\mathbb{A}, \mathbb{C}) \in \overline{\mathcal{Y}}_{(\alpha,\beta^*)}$ outperforms strategy $\mathcal{P}^*$ if

$$\begin{aligned} \mathbb{A} &\geq \widehat{\mathbb{A}} \\ \mathbb{C} &\geq \widehat{\mathbb{C}} \ , \end{aligned} \tag{6.19}$$

where one of the inequalities in equation (6.19) is strict.

Remark 6.2 (Other outperformance percentiles)**.** *We have restricted attention to $\mathcal{Y}_{(\alpha,\beta^*)}$ such that β^* corresponds to the median of the benchmark strategy. We can obviously select other choices based on other percentiles, which are a result of any admissible strategy. However, the median would be a common choice.*

6.2 Candidate outperformance strategy

In the following, we rely on Lemma 6.1, since we require that $(\mathbb{A}(\kappa), \mathbb{C}(\kappa)) \in \mathcal{S}_\kappa(\mathcal{Y}_{(\alpha,\beta^*)})$ exists $\forall \kappa > 0$. We also use the shorthand notation

$$\begin{aligned} (\mathbb{A}(0^+), \mathbb{C}(0^+)) &= \lim_{\kappa \to 0^+} (\mathbb{A}(\kappa), \mathbb{C}(\kappa)) \\ (\mathbb{A}(\infty), \mathbb{C}(\infty)) &= \lim_{\kappa \to \infty} (\mathbb{A}(\kappa), \mathbb{C}(\kappa)) \ . \end{aligned} \tag{6.20}$$

These limits both exist from Lemma 6.1 and Lemma 6.2. In the following, when we use the notation $\kappa = 0^+$ or $\kappa = \infty$, it is to be understood in the sense of equation (6.20). We make the following assumption.

Assumption 6.1. *Given a benchmark strategy $(\widehat{\mathbb{A}}, \widehat{\mathbb{C}}) \in \overline{\mathcal{Y}}_{(\alpha,\beta^*)}$, then $\exists \kappa_{\max} > 0$ such that for a point $(\mathbb{A}(\kappa_{\max}), \mathbb{C}(\kappa_{\max})) \in \mathcal{S}_{\kappa_{\max}}(\mathcal{Y}_{(\alpha,\beta^*)})$, $\mathbb{A}(\kappa_{\max}) \geq \widehat{\mathbb{A}}$.*

Remark 6.3. *A value of $\kappa_{\max}$ is usually easily found in practice by examining extreme values of κ. The existence of this point will allow us to restrict attention to $\kappa \in (0, \kappa_{\max}]$ in our search for outperformance strategies. If Assumption 6.1 does not hold, then we have the degenerate case that the only possible outperformance point is $(\mathbb{A}(\infty), \mathbb{C}(\infty))$.*

We can now focus on a subset of $\mathbb{P}$ in our search for an outperformance strategy. Given $\kappa_{\max}$ from Assumption 6.1, we define $\widehat{\mathbb{P}}$,

$$\widehat{\mathbb{P}} = \{(\mathbb{A}, \mathbb{C}) \in \mathbb{P} : \mathbb{A}(0^+) \leq \mathbb{A} \leq \mathbb{A}(\kappa_{\max})\} \ . \tag{6.21}$$

Similarly, we can restrict attention to a subset of $\mathcal{S}(\mathcal{Y}_{\alpha,\beta^*})$, and $\mathcal{Y}_{\alpha,\beta^*}$

$$\begin{aligned} \widehat{\mathcal{S}}(\mathcal{Y}_{\alpha,\beta^*}) &= \{(\mathbb{A}, \mathbb{C}) \in \mathcal{S}(\mathcal{Y}_{\alpha,\beta^*}) : \mathbb{A}(0^+) \leq \mathbb{A} \leq \mathbb{A}(\kappa_{\max})\} \\ \widehat{\mathcal{Y}}_{\alpha,\beta^*} &= \{(\mathbb{A}, \mathbb{C}) \in \mathcal{Y}_{\alpha,\beta^*} : \mathbb{A}(0^+) \leq \mathbb{A} \leq \mathbb{A}(\kappa_{\max})\} \ . \end{aligned} \tag{6.22}$$

Given a benchmark strategy which generates $(\widehat{\mathbb{A}}, \widehat{\mathbb{C}})$, Algorithm 6.1 is used to generate a candidate point $(\mathbb{A}(\kappa^*), \mathbb{C}(\kappa^*))$ on the Ambition-CVAR frontier which potentially outperforms the benchmark, in terms of Definition 6.4. Algorithm 6.1 uses bisection to find the smallest value of κ such

Require: Function which returns $(\mathbb{A}(\kappa), \mathbb{C}(\kappa))$ on Ambition-CVAR frontier.

input: $(\widehat{\mathbb{A}}, \widehat{\mathbb{C}})$ from benchmark ; *tol*
input: $\kappa_{\max}$ from Assumption 6.1
$\kappa_{\min} = 0, \kappa_* = \kappa_{\max}$
loop
  {Uses monotonicity Equation 6.7 }
  $\kappa_{test} := (\kappa_* + \kappa_{\min})/2$
  if $(\mathbb{A}(\kappa_{test}) < \widehat{\mathbb{A}})$ **then**
    $\kappa_{\min} = \kappa_{test}$
  else
    $\kappa_* = \kappa_{test}$
  end if
  if $(|\kappa_* - \kappa_{\min}| < \text{tol})$ **then**
    break
  end if
end loop

if $\Big((\mathbb{C}(\kappa_*) > \widehat{\mathbb{C}}) \text{ or } (\mathbb{A}(\kappa_*) > \widehat{\mathbb{A}}) \Big) \text{ and } \Big((\mathbb{C}(\kappa_*) \geq \widehat{\mathbb{C}}) \text{ and } (\mathbb{A}(\kappa_*) \geq \widehat{\mathbb{A}}) \Big)$ **then**
  found := true
else
  found := false
end if
Return ($(\mathbb{A}(\kappa_*), \mathbb{C}(\kappa_*))$, found)

ALGORITHM 6.1: *Candidate outperformance point on Ambition-CVAR efficient frontier.*

that $\mathbb{A}(\kappa^+) \geq \widehat{\mathbb{A}}$, to within a numerical tolerance. The bisection algorithm uses the monotonicity properties of Lemma 6.2, hence must terminate. This algorithm will generate a point satisfying the outperformance criteria in Definition 6.4 (to within a numerical tolerance), if such a point exists in $\widehat{\mathcal{S}}(\mathcal{Y}_{\alpha,\beta^*})$.

Recall that $\mathcal{S}(\mathcal{Y}_{\alpha,\beta^*}) \subseteq \mathbb{P}$ where $\mathbb{P}$ is set of Pareto optimal points. Hence there may be points in $\widehat{\mathbb{P}} \notin \widehat{\mathcal{S}}(\mathcal{Y}_{\alpha,\beta^*})$ which outperform the benchmark, but cannot be found by scalarization. For ease of exposition, we have the following geometric characterization of the case where all points in $\widehat{\mathbb{P}}$ can be found by scalarization.

Property 6.1 ($\widehat{\mathbb{P}} = \widehat{\mathcal{S}}(\mathcal{Y}_{\alpha,\beta^*})$)**.** *If all points in $\widehat{\mathbb{P}}$ have supporting hyperplanes w.r.t. $\mathcal{Y}_{(\alpha,\beta^*)}$, then $\widehat{\mathbb{P}} = \widehat{\mathcal{S}}(\mathcal{Y}_{\alpha,\beta^*})$.*

Remark 6.4 (Sufficient condition for Property 6.1)**.** *If $\mathcal{Y}_{(\alpha,\beta^*)}$ is convex, then all points in $\mathbb{P}$ (hence $\widehat{\mathbb{P}}$) have supporting hyperplanes. However, Property 6.1 allows more general cases.*

Consider the case where the benchmark strategy is not Pareto optimal, i.e. $(\widehat{\mathbb{A}}, \widehat{\mathbb{C}}) \notin \widehat{\mathbb{P}}$. Otherwise, outperformance is impossible by definition.

Proposition 6.2 (Outperformance point and Algorithm 6.1)**.** *Suppose Property 6.1 holds, $(\widehat{\mathbb{A}}, \widehat{\mathbb{C}}) \notin \widehat{\mathbb{P}}$, and $(\widehat{\mathbb{A}}, \widehat{\mathbb{C}})$ satisfies Assumption 6.1, then Algorithm 6.1 will generate κ_*, such that*

$$\lim_{\kappa \downarrow \kappa_*} (\mathbb{A}(\kappa), \mathbb{C}(\kappa)) \quad = \quad (\mathbb{A}(\kappa_*^+), \mathbb{C}(\kappa_*^+)) \ , \tag{6.23}$$

outperforms the benchmark $(\widehat{\mathbb{A}}, \widehat{\mathbb{C}})$ as in Definition 6.4.

Proof. Since $(\widehat{\mathbb{A}}, \widehat{\mathbb{C}}) \notin \widehat{\mathbb{P}}$, then, from Property 6.1, and the definition of Pareto optimality, $\exists \hat{\kappa} > 0$, such that $((\mathbb{A}(\hat{\kappa}), \mathbb{C}(\hat{\kappa})) \in \mathcal{S}(\mathcal{Y}_{\alpha,\beta^*})$ outperforms the benchmark in the sense of Definition 6.4. From the monotonicity properties of Lemma 6.2 and Property 6.1, it follows that $\exists \kappa' \in [0, \kappa_{\max}]$, such that $((\mathbb{A}(\kappa'), \mathbb{C}(\kappa')) \in \widehat{\mathcal{S}}(\mathcal{Y}_{\alpha,\beta^*})$ satisfies one of

(i) $\mathbb{A}(\kappa') \geq \widehat{\mathbb{A}} \;\; ; \;\; \mathbb{C}(\kappa') > \widehat{\mathbb{C}}$,

(ii) $\mathbb{A}(\kappa') > \widehat{\mathbb{A}} \;\; ; \;\; \mathbb{C}(\kappa') \geq \widehat{\mathbb{C}}$,

(iii) $\mathbb{A}(\kappa') > \widehat{\mathbb{A}} \;\; ; \;\; \mathbb{C}(\kappa') > \widehat{\mathbb{C}}$.

Noting that $\mathbb{A}(\kappa_{\max}) \geq \widehat{\mathbb{A}}$, (from Assumptions 6.1), the monotonicity properties of Lemma 6.2, and the fact that all points in $\widehat{\mathbb{P}}$ have supporting hyperplanes, then the existence of this $\kappa' \in (0, \kappa_{\max}]$ implies the smallest $\kappa_* \in (0, \kappa']$ such that $\mathbb{A}(\kappa_*^+) \geq \widehat{\mathbb{A}}$ has the property that $(\mathbb{A}(\kappa_*^+), \mathbb{C}(\kappa_*^+))$ satisfies one of (i-iii) above. □

Remark 6.5 (Assumption that $(\widehat{\mathbb{A}}, \widehat{\mathbb{C}}) \notin \widehat{\mathbb{P}}$.)**.** *In Proposition 6.2 we have assumed that $(\widehat{\mathbb{A}}, \widehat{\mathbb{C}}) \notin \widehat{\mathbb{P}}$. If this is not the case, then if Property 6.1 holds, we have the trivial case that Algorithm 6.1 simply returns $(\widehat{\mathbb{A}}, \widehat{\mathbb{C}})$, i.e. outperformance is impossible, since $(\widehat{\mathbb{A}}, \widehat{\mathbb{C}})$ is already Pareto optimal under Ambition-CVAR criteria.*

Remark 6.6 ($\min \kappa_*$ s.t. $\mathbb{A}(\kappa_*^+) \geq \widehat{\mathbb{A}}$)**.** *Our objective is to find κ_* s.t. $\mathbb{A}(\kappa_*^+) = \widehat{\mathbb{A}}$, since in this case we have*

(i) The optimal strategy has the same median value of terminal wealth.

(ii) For this value of median terminal wealth, the optimal strategy has the largest possible value of $CVAR_\alpha$.

This point is then Median-CVAR optimal.

Remark 6.7 (Possible failure of Algorithm 6.1)**.** *We have no guarantee that Property 6.1 holds, since it is not obvious that $\mathcal{Y}_{(\alpha,\beta^*)}$ satisfies the sufficient conditions which guarantee that Algorithm 6.1 succeeds (i.e. finds an outperformance point). However, in practice, we have not observed failure.*

Figure 6.1 illustrates this concept. For an arbitrary fixed value of Ambition level β, by varying κ, we can trace out the Ambition-CVAR efficient frontier $\mathcal{S}(\mathcal{Y}_{\alpha,\beta})$. Suppose we choose $\beta = \beta^*$, which is the median of the benchmark strategy. If we can find a κ such that $\mathbb{A}(\kappa_*^+) = \widehat{\mathbb{A}} = 0.5$ than the strategy which generates this point on the Ambition-CVAR frontier is also Median-CVAR optimal. In other words, for this fixed value of a benchmark median, there is no other strategy which generates a larger CVAR.

Remark 6.8 (Median-CVAR efficiency)**.** *Suppose that Algorithm 6.1 succeeds, and $\mathbb{A}(\kappa_*^+) = \widehat{\mathbb{A}} = 0.5$. Then, we have the case illustrated in Figure 6.1. This is a Median-CVAR optimal point (given this median value, no other strategy has a larger CVAR). However, this point is not necessarily Median-CVAR efficient, i.e. it may not be a Pareto optimal point, with criteria Median and CVAR. A sufficient condition for the Median-CVAR optimal point to be Median-CVAR efficient, is that the achievable Median-CVAR objective set is convex.*

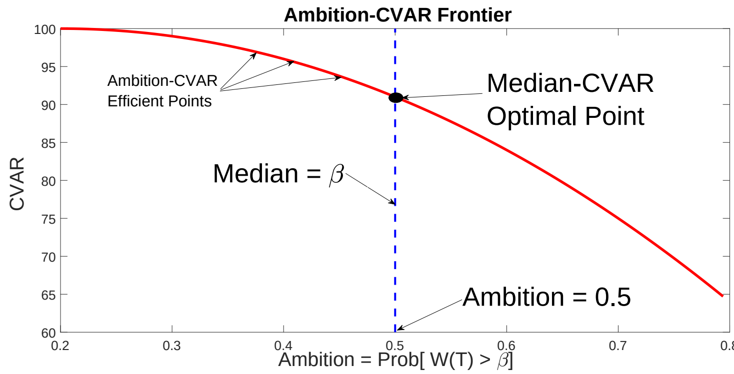

FIGURE 6.1: *Conceptual diagram of an efficient Ambition-CVAR frontier. The point on the frontier having Ambition* $= Pr[W_T > \beta] = 0.5$ *corresponds to a Median-CVAR optimal point, with* $Median[W_T] = \beta$.

If the pre-conditions for Proposition 6.1 hold, then the point $(\mathbb{A}(\kappa_*^+), \mathbb{C}(\kappa_*^+))$ outperforms the benchmark point $(\widehat{\mathbb{A}}, \widehat{\mathbb{C}})$. Hence the strategy $\mathcal{P}(\cdot)$ is to be preferred over the benchmark strategy. However, from Remark 6.8, we learn that it is possible that there may be another strategy, which generates a point on the Median-CVAR frontier, which dominates the point $(\mathbb{A}(\kappa_*^+), \mathbb{C}(\kappa_*^+))$. In this case, this other strategy would be preferred over the strategy $\mathcal{P}(\cdot)$.

In principle, we could construct an approximate Median-CVAR efficient frontier in the following manner. As a first step, we need to generate a set of feasible Median values $\hat{\beta}$. One way to do this would to use a constant proportion strategy, for a range of values of equity fraction $p \in [0,1]$. For each value of $\beta \in \hat{\beta}$, we would run Algorithm 6.1, to generate point $(\mathbb{A}(\kappa_*^+), \mathbb{C}(\kappa_*^+))$. If $\mathbb{A}(\kappa_*^+) = .5$, then this is a point in the achievable Median-CVAR objective set. The points on the Median-CVAR efficient frontier are then given by the upper right boundary of the convex hull of these points. This, of course, would be a computationally expensive exercise.

We also note that if Property 6.1 holds, $\mathbb{A}(\kappa_*^+) = 0.5$ and the achievable Median-CVAR objective set is convex, then the point returned from Algorithm 6.1 is both Median-CVAR optimal and Median-CVAR efficient.

Nevertheless, we remind the reader that, given the pre-conditions for Proposition 6.1, the strategy returned from Algorithm 6.1 outperforms the benchmark strategy, in terms of the Median-CVAR criteria. This was our original objective.

7 Pre-commitment Ambition-CVAR

We will now pose the problem of determining points in $\mathcal{S}_\kappa(\mathcal{Y}_{(\alpha,\beta)})$ in a form which is amenable to solution by optimal stochastic control techniques. Using the definitions in equation (6.1), we can rewrite equation (6.3) as a control problem. For a given scalarization parameter κ and intervention times t_n, the pre-commitment Ambition-CVAR problem $(PCAC_{t_0}(\kappa))$ is given in terms of the value function $J(s,b,t_0^-)$,

$$(PCAC_{t_0}(\kappa)): \qquad J\left(s,b,t_0^-\right) = \sup_{\mathcal{P}_0 \in \mathcal{A}} \sup_{W^*} \Bigg\{ E_{\mathcal{P}_0}^{X_0^+,t_0^+} \Bigg[W^* + \frac{1}{\alpha} \min(W_T - W^*, 0) + \kappa \mathbf{1}_{W_T > \beta} \Bigg| X(t_0^-) = (s,b) \Bigg] \Bigg\} \tag{7.1}$$

$$\text{subject to} \quad \begin{cases} (S_t, B_t) \text{ follow processes (2.3) and (2.4); } \quad t \notin \mathcal{T} \\ W_\ell^+ = S(t_\ell^-) + B(t_\ell^-) + q_\ell\, ; \;\; X_\ell^+ = (S_\ell^+, B_\ell^+) \\ S_\ell^+ = p_\ell(\cdot) W_\ell^+\, ; \;\; B_\ell^+ = (1 - p_\ell(\cdot)) W_\ell^+ \\ p_\ell(\cdot) \in \mathcal{Z} = [0,1]\, ; \;\; \text{if } W_\ell^+ > 0 \\ p_\ell = 0\, ; \;\; \text{if } W_\ell^+ \leq 0 \\ \ell = 0, \ldots, M-1\, ; \;\; t_\ell \in \mathcal{T} \end{cases} . \tag{7.2}$$

Interchange the sup sup in equation (7.1), so that value function $J\left(s,b,t_0^-\right)$ can be written as

$$J\left(s,b,t_0^-\right) = \sup_{W^*} \sup_{\mathcal{P}_0 \in \mathcal{A}} \left\{ E_{\mathcal{P}_0}^{X_0^+,t_0^+} \left[W^* + \frac{1}{\alpha} \min(W_T - W^*,0) + \kappa \mathbf{1}_{W_T > \beta} \middle| X(t_0^-) = (s,b) \right] \right\} . \tag{7.3}$$

Noting that the inner supremum in equation (7.3) is a continuous function of W^*, and assuming that the domain of W^* is compact, then define

$$\mathcal{W}^*(s,b) = \arg\max_{W^*} \left\{ \sup_{\mathcal{P}_0 \in \mathcal{A}} \left\{ E_{\mathcal{P}_0}^{X_0^+,t_0^+} \left[W^* + \frac{1}{\alpha} \min(W_T - W^*,0) + \kappa \mathbf{1}_{W_T > \beta} \middle| X(t_0^-) = (s,b) \right] \right\} \right\} . \tag{7.4}$$

Denote the investor's initial wealth at t_0 by W_0. Then we have the following result.

Proposition 7.1 (Pre-commitment strategy equivalence to a time consistent policy for an alternative objective function)**.** *The pre-commitment Ambition-CVAR strategy $\mathcal{P}^*$ determined by solving $J(0, W_0, t_0^-)$ (with $\mathcal{W}^*(0, W_0)$ from equation (7.4)) is the time consistent strategy for the equivalent problem TCEQ (with fixed $\mathcal{W}^*(0,W_0)$ and β), with value function $\tilde{J}(s,b,t)$ defined by*

$$(TCEQ_{t_n}(\kappa\alpha)): \qquad \tilde{J}\left(s,b,t_n^-\right) = \sup_{\mathcal{P}_n \in \mathcal{A}} \Bigg\{ E_{\mathcal{P}_n}^{X_n^+,t_n^+} \Bigg[\min(W_T - \mathcal{W}^*(0, W_0),0) + (\kappa\alpha) \mathbf{1}_{W_T > \beta} \Bigg| X(t_n^-) = (s,b) \Bigg] \Bigg\} . \tag{7.5}$$

Proof. Combining equations (7.3) and (7.4) we have that

$$J\left(0,W_0,t_0^-\right) = \sup_{\mathcal{P}_0 \in \mathcal{A}} \Bigg\{ E_{\mathcal{P}_0}^{X_0^+,t_0^+} \Bigg[\mathcal{W}^*(0,W_0) + \frac{1}{\alpha} \min(W_T - \mathcal{W}^*(0,W_0),0) + \kappa \mathbf{1}_{W_T > \beta} \Bigg| X(t_0^-) = (0,W_0) \Bigg] \Bigg\} . \tag{7.6}$$

while evaluating equation (7.5) at t_0 with initial wealth $W_0 = B_0$ gives

$$\tilde{J}\left(0,W_0,t_0^-\right) = \sup_{\mathcal{P}_0 \in \mathcal{A}} \left\{ E_{\mathcal{P}_0}^{X_0^+,t_0^+} \left[\min(W_T - \mathcal{W}^*(0, W_0),0) + (\kappa\alpha) \mathbf{1}_{W_T > \beta} \middle| X(t_0^-) = (0,W_0) \right] \right\} . \tag{7.7}$$

Since $\alpha > 0$ and $\mathcal{W}^*(0, W_0)$ can be regarded as a constant, then any control $\mathcal{P}^*$ which maximizes equation (7.6) also maximizes equation (7.7). With a fixed value of $\mathcal{W}^*(0,W_0)$, the objective function (7.5) is a simple expectation, hence we can determine $\mathcal{P}_n^*$ by dynamic programming, which is clearly time consistent. $\square$

Remark 7.1 (An Implementable Strategy)**.** *Given an initial level of wealth W_0 at t_0, then the optimal control for the pre-commitment problem (7.1) is the same optimal control for the time consistent problem $(TCEQ_{t_n}(\kappa\alpha))$ (7.5), $\forall t > 0$. Hence we can regard problem $(TCEQ_{t_n}(\kappa\alpha))$ as the* Ambition-CVAR induced time consistent strategy*. See Strub et al. (2019) for a discussion of induced time consistent strategies.*

We can alternatively regard time consistent strategy $(TCEQ_{t_n}(\kappa\alpha))$ as our basic objective function. $\mathcal{W}^*(0,W_0)$ is a fixed disaster level of terminal wealth, which is set at time zero. Solution of the pre-commitment Ambition-CVAR problem merely determines a reasonable value for the parameter $\mathcal{W}^*(0,W_0)$. As a by-product of computing the optimal pre-commitment Ambition-CVAR strategy, we also determine the optimal control for the induced time consistent strategy. Hence the induced strategy is implementable, in the sense that the investor has no incentive to deviate from the strategy computed at time zero, at later times (Forsyth, 2020).

8 Algorithm for Pre-commitment Ambition-CVAR

8.1 Formulation

In order to solve problem $(PCAC_{t_0}(\kappa))$, our starting point is equation (7.3), where we have interchanged the $\sup\sup(\cdot)$ in equation (7.1). We expand the state space to $\hat{X} = (s,b,W^*)$, and define the auxiliary function $V(s, b, W^*, t)$

$$V(s, b, W^*, t_n^-) = \sup_{\mathcal{P}_n \in \mathcal{A}} \left\{ E_{\mathcal{P}_n}^{\hat{X}_n^+, t_n^+} \left[W^* + \frac{1}{\alpha} \min((W_T - W^*),0) + \kappa \mathbf{1}_{W_T > \beta} \middle| \hat{X}(t_n^-) = (s,b,W^*) \right] \right\} . \tag{8.1}$$

$$\text{subject to} \quad \begin{cases} (S_t, B_t) \text{ follow processes (2.3) and (2.4)}; \quad t \notin \mathcal{T} \\ w_\ell^+ = s + b + q_\ell \,;\ \hat{X}_\ell^+ = (S_\ell^+, B_\ell^+, W^*) \\ S_\ell^+ = p_\ell(\cdot) w_\ell^+ \,;\ B_\ell^+ = (1 - p_\ell(\cdot)) w_\ell^+ \\ p_\ell(\cdot) \in \mathcal{Z} = [0,1] \ ; \ \text{ if } w_\ell^+ > 0 \\ p_\ell = 0 \ ; \ \text{ if } w_\ell^+ \le 0 \\ \ell = 0, \ldots, M-1 \ ; \ t_\ell \in \mathcal{T} \end{cases} . \tag{8.2}$$

Equation (8.1) is a simple expectation. Hence we can solve this auxiliary problem using dynamic programming. The optimal control $p_n(w,W^*)$ at time t_n is then determined from

$$p_n(w, W^*) = \begin{cases} \underset{p' \in \mathcal{Z}}{\arg\max}\, V(wp', w(1-p'), W^*, t_n^+), & w > 0 \\ 0, & w \le 0 \end{cases} . \tag{8.3}$$

The solution is advanced (backwards) across time t_n by

$$\begin{aligned} V(s, b, W^*, t_n^-) &= V(w^+ p_n(w^+, W^*), w^+(\ 1 - p_n(w^+, W^*)\ ), W^*, t_n^+) \\ & \qquad w^+ = s + b + q_n \ . \end{aligned} \tag{8.4}$$

At $t = T$, we have

$$V(s, b, W^*) \;\;=\;\; W^* + \frac{\min((s + b - W^*), 0)}{\alpha} + \kappa \mathbf{1}_{(s+b)>\beta} \; . \tag{8.5}$$

For $t \in (t_{n-1}, t_n)$, there are no cash flows, discounting (all quantities are inflation adjusted), or controls applied. Hence the tower property gives for $0 < h < (t_n - t_{n-1})$

$$V(s,b,W^*,t) \;\;=\;\; E\Big[V(S(t+h), B(t+h), W^*, t+h) \big| S(t) = s, B(t) = b \Big] \; ; \; t \in (t_{n-1}, t_n - h) \; . \tag{8.6}$$

Applying Ito's Lemma for jump processes (Tankov and Cont, 2009), noting equations (2.3) and (2.4), and letting $h \to 0$ gives, for $t \in (t_{n-1}, t_n)$

$$\begin{aligned} &V_t + \frac{(\sigma^s)^2 s^2}{2} V_{ss} + (\mu^s - \lambda_\xi^s \zeta^s) s V_s + \lambda_\xi^s \int_{-\infty}^{+\infty} V(e^y s, b, t) f^s(y) \; dy \\ &\quad + \frac{(\sigma^b)^2 b^2}{2} V_{bb} + (\mu^b - \lambda_\xi^b \zeta^b) b V_b + \lambda_\xi^b \int_{-\infty}^{+\infty} V(s, e^y b, t) f^b(y) \; dy \\ &\quad - (\lambda_\xi^s + \lambda_\xi^b) V + \rho_{sb} \sigma^s \sigma^b s b V_{sb} \\ &= 0 \; . \end{aligned} \tag{8.7}$$

Proposition 8.1 (Equivalence of formulation (8.1-8.7) to problem $(PCAC_{t_0}(\kappa))$)**.** *Define*

$$J(s,b,t_0^-) = \sup_{W'} V(s,b,W',t_0^-) \; , \tag{8.8}$$

then formulation (8.1-8.7) is equivalent to problem $(PCAC_{t_0}(\kappa))$.

Proof. Replace $V(s,b,W',t_0^-)$ in equation (8.8) by the expressions in equations (8.1-8.7). Begin with equation (8.5), and recursively work backwards in time, then we obtain equations (7.1-7.2), by interchanging sup sup in the final step. ☐

8.2 Numerical Algorithm: $(PCAC_{t_0}(\kappa))$

8.2.1 Solution of Auxiliary Problem

We begin by solving the auxiliary problem (8.1-8.2), with a fixed value of W^* and β. We do not allow shorting of stock, so the amount in the stocks $S(t) \geq 0$. We discretize the state space in $s > 0$ using $n_{\hat{x}}$ equally spaced nodes in the $\hat{x} = \log s$ direction, on a finite localized domain $s \in [e^{\hat{x}_{\min}}, e^{\hat{x}_{\max}}]$. The investor can become insolvent due to withdrawals, which means that short positions in the bond are mathematically possible. We consider two cases. We discretize the state space in $b > 0$ using n_y equally spaced nodes in the $y = \log b$ direction, on a finite localized domain $b \in [b_{\min}, b_{\max}] = [e^{y_{\min}}, e^{y_{\max}}]$. We also define a $b' > 0$ grid, using n_b equally spaced nodes in the $y' = \log b'$ direction, on the localized domain with $b' \in [b'_{\min}, b'_{\max}] = [e^{y_{\min}}, e^{y_{\max}}]$. The grid $[s_{\min}, s_{\max}] \times [b_{\min}, b_{\max}]$ represents cases where $b \geq 0$. The grid $[s_{\min}, s_{\max}] \times [b'_{\min}, b'_{\max}]$ represents cases where $b = -b' < 0$.

Note that PIDE (8.7) has the same form on the b and b' grids. The PIDE degenerates in the domain $[s_{\min}, s_{\max}] \times [b'_{\min}, b'_{\max}]$, due to the insolvency condition (3.7). In principle, we can use this auxiliary b' grid to handle cases where we allow leverage, but we do not exploit this in this work.

We use the Fourier methods discussed in Forsyth and Labahn (2019) to solve PIDE (8.7) between rebalancing times. To minimize localization errors and wrap-around errors, we extend the computational domain for $s < s_{\min}$, $s > s_{\max}$ and assume a constant value for the solution in the extended domain as described in Forsyth and Labahn (2019). This effectively adds artificial boundary conditions on the localized domain boundary. This localization error can be made small by selecting $|x_{\min}|, x_{\max}$ sufficiently large. A similar approach is used in the b direction.

We choose the localized domain $[\hat{x}_{\min}, \hat{x}_{\max}] = [\log(10^2) - 8, \log(10^2) + 8]$, with $[y_{\min}, y_{\max}] = [\hat{x}_{\min}, \hat{x}_{\max}]$ (units thousands of dollars). In our numerical experiments, we carried out tests replacing $[\hat{x}_{\min}, \hat{x}_{\max}]$ by $[\hat{x}_{\min} - 2, \hat{x}_{\max} + 2]$ and similarly replacing $[y_{\min}, y_{\max}]$ by $[y_{\min} - 2, y_{\max} + 2]$. In all cases, this resulted in changes to the summary statistics in at most the fifth digit, verifying that the localization error is small.

At rebalancing times, we discretize the equity fraction $p \in [0,1]$ using n_y equally spaced nodes, and then evaluate the right hand side of equation (8.4) using linear interpolation. We then solve the optimization problem (8.4) using exhaustive search over the discretized p values.

8.2.2 Outer Optimization over W^*

Given an approximate solution of the auxiliary problem (8.1-8.2) at $t = 0$, which we denote by $V(s, b, W^*, 0)$, we then determine the final solution for problem $PCAC_{t_0}(\kappa)$) in equations (7.1-7.2) using equation (8.8). More specifically, we solve

$$\begin{aligned} J(0, W_0, 0^-) \quad &= \quad \sup_{W'} V(0, W_0, W', 0^-) \\ &\quad\; W_0 = \text{ initial wealth } . \end{aligned} \tag{8.9}$$

We solve the auxiliary problem on sequence of grids $n_{\hat{x}} \times n_y$. On the coarsest grid, we discretize W^* and solve problem (8.9) by exhaustive search. We use this optimal value of W^* as a starting point to a one dimensional optimization algorithm on a sequence of finer grids. Note that each iteration of the one dimensional optimization solver requires a complete solve of the auxiliary PIDE problem.

This approach does not guarantee that we have the globally optimal solution to problem (8.9), since the problem is not guaranteed to be convex. However, we have made a few tests by carrying out a grid search on the finest grid, which suggest that we do indeed have the globally optimal solution.

9 Median-CVAR Optimization

We first determine a target median value β^* from the benchmark strategy. We then fix $\beta = \beta^*$ for problem $(PCAC_{t_0}(\kappa))$ in equation (7.1). We then use Algorithm 6.1 to determine κ such that

$$\mathbb{A}(\kappa^+) \quad \geq \quad \mathrm{A}^{x_0,0}_{\mathcal{P}^*(\cdot)} = E^{X_0^+, t_0^+}_{\mathcal{P}_0^*}[\mathbf{1}_{W_T > \beta^*}] = 0.5 \ . \tag{9.1}$$

If Algorithm 6.1 succeeds, then we have determined the strategy which outperforms the benchmark strategy, in the sense of Definition 6.4. If, in addition, $\mathbb{A}(\kappa^+) = \widehat{\mathbb{A}} = 0.5$, then we have found the strategy which maximizes CVAR_α for this fixed value of the benchmark median. This is a point which is Median-CVAR optimal. However, this point may not be Median-CVAR efficient, as noted in Remark 6.8.

Method	μ^s	σ^s	λ^s	p^s_{up}	η^s_1	η^s_2	ρ_{sb}
			Real CRSP Value-Weighted Index				
threshold ($\theta = 3$)	.08607	.14600	.32258	0.23333	4.3578	5.5089	(see below)
GBM	.08044	.18460	N/A	N/A	N/A	N/A	(see below)
Method	μ^b	σ^b	λ^b	p^b_{up}	η^b_1	η^b_2	ρ_{sb}
			Real 10-year Treasury				
threshold ($\theta = 3$)	.0236	.05380	.3871	.6111	16.178	17.279	.0510
GBM	.0228	.06528	N/A	N/A	N/A	N/A	.0823
			30 day T-bill				
threshold ($\theta = 3$)	.00454	.01301	.5161	0.3958	65.875	57.737	.08311
GBM	.00448	.01814	N/A	N/A	N/A	N/A	.0587

TABLE 10.1: *Estimated annualized parameters for double exponential jump diffusion model. Value-weighted CRSP index, 10-year Treasury, 30 day T-bill, deflated by the CPI. Sample period 1926:1 to 2018:12. GBM refers to the assumption of a Geometric Brownian Motion model (no jumps). Threshold method described in Appendix A.*

9.1 Equivalent Time Consistent Strategy

We remind the reader that our Median-CVAR optimal solution is actually a special case of the Pre-commitment Ambition-CVAR control from problem ($PCAC_{t_0}(\kappa)$) described in Section 7, which is not time consistent. However, from Proposition 7.1, we learn that this control, as seen at time zero, is identical to the control for the time consistent problem ($TCEQ_{t_n}(\kappa\alpha)$) given in equation (7.5). Hence we can view our optimal control as the time consistent control for objective function (7.5), as long as we fix the values of W^* and β for all times $t > 0$. Consequently, this strategy is implementable. We have argued in Forsyth (2020) that this approach does, in fact, lead to more reasonable strategies, compared to the naive approach of forcing time consistency, in the case of Mean-CVAR optimization.

10 Data

We use the threshold technique (Mancini, 2009; Cont and Mancini, 2011; Dang and Forsyth, 2016) to estimate the parameters for the parametric stochastic process models. A brief overview of this method is given in Appendix A. Note that the data is inflation adjusted, so that all parameters reflect real returns. Table 10.1 shows the results of calibrating the models to the historical data. Using the 10 year treasuries as the bond index, the algorithm identified 30 total jumps in the stock time series, and 36 jumps in the bond time series. Only one of the jump times was common to both series. The stock series had many jumps in the 1930s and the bond series had many jumps in the 1980s. In the threshold case, the correlation ρ_{sb} is computed by removing any returns which occur at times corresponding to jumps in either series, and then using the sample covariance.

As a point of comparison, we also show the estimated parameters for the time series assuming Geometric Brownian Motion (GBM) for both series. Maximum Likelihood was used to obtain the GBM estimates.

Investment horizon (years)	45
Equity market index	Real CRSP US market index
Bond asset index	Real 1-month T-bill
	Real 10-year Treasury
Initial investment W_0	500
Real investment each year	20.0 ($0 \leq t_i \leq 15$), -40.0 ($16 \leq t_i \leq 45$)
Rebalancing interval (years)	1

TABLE 11.1: *Input data for examples. Cash is invested at $t_i = 0,1,\ldots,15$ years, and withdrawn at $t_i = 16,17,\ldots,45$ years. Units for real investment: thousands of dollars. Parameters determined from CRSP data, 1926:1-2018:12. Deflated using the US CPI.*

11 Investment Scenario

Table 11.1 shows our investment scenario. To give a concrete example of where this scenario applies, consider the following situation. We imagine a 50-year old investor, who has saved $500,000 in a defined contribution (DC) pension plan account. It is assumed that the DC pension plan account is tax advantaged, and no taxes are paid except on withdrawals.

This investor is currently employed in a stable industry, and earns about $100,000 per year. The total employee-employer contributions to his DC plan are assumed to total 20% of his salary. We assume that the investor's real salary will remain roughly constant in real terms over the next 15 years, hence he can expect total contributions of $20,000 per year (real) until he retires at age 65. The investor then plans to withdraw $40,000 per year (real) after retiring. This amount will be augmented from various government programs, which will generate $20,000 per year, hence the total pension will replace about 60% of pre-retirement salary. The investor plans to make withdrawals for 30 years. In the case of a Canadian male of age 65, there is only a probability of 0.13 that this person will still be alive at age 95. Given that we have ruled out the use of annuities, is seems reasonable for the investor to assume a fixed, lengthy period of withdrawals. Hence the assumption of 30 years of withdrawals arguably provides a reasonable (but not perfect) buffer against unexpected longevity. As an additional longevity hedge, our investment strategy typically targets a significant median value of final wealth (at 30 years). Note that this scenario is based on both a late accumulation phase, and the decumulation phase, hence the optimal investment strategy will clearly be a function of time and wealth level.

In the following, we will use thousands as our units of wealth, so that, for example, the investor injects 20.0 per year into the portfolio, and withdraws 40.0 per year.

We ignore labour income risk. Many studies assume that real earnings are expected to follow a hump-shaped pattern, rising rapidly until about age 35, then more slowly until around age 45-50, and slowly declining thereafter (see, e.g. Cocco et al., 2005; Blake et al., 2014). It is common to add diffusive shocks to this trend, though Cocco et al. (2005) calculate that the utility costs of assuming labour income has no risk are not high. The hump-shaped pattern described above has been questioned recently by Rupert and Zanella (2015), who find wage rates do not decline prior to retirement. Average income does fall on average during those years, but this is due to a reduction in hours worked by some employees transitioning into retirement.

Data series	Optimal expected block size $\hat{b}$ (months)
Real 10-year Treasury index	4.1
Real CRSP value-weighted index	3.0
Real 30 day T-bill	50.2

TABLE 11.2: *Optimal expected blocksize $\hat{b} = 1/v$ when the blocksize follows a geometric distribution $Pr(b = k) = (1 - v)^{k-1}v$. The algorithm in Patton et al. (2009) is used to determine $\hat{b}$.*

11.1 Synthetic Market

We fit the parameters for the parametric stock and bond processes (2.3 - 2.4) as described in Section 10 and Appendix A. We then compute and store the optimal controls based on the parametric market model. Finally, we compute various statistical quantities by using the stored control, and then carrying out Monte Carlo simulations, based on processes (2.3 - 2.4).

11.2 Historical Market

We compute and store the optimal controls based on the parametric model (2.3-2.4) as for the synthetic market case. However, we compute statistical quantities using the stored controls, but using bootstrapped historical return data directly. We remind the reader that all returns are inflation adjusted. We use the stationary block bootstrap method (Politis and Romano, 1994; Politis and White, 2004; Patton et al., 2009; Dichtl et al., 2016). A crucial parameter is the expected blocksize. Sampling the data in blocks accounts for serial correlation in the data series. We use the algorithm in (Patton et al., 2009) to determine the optimal blocksize for the bond and stock returns separately. The results are shown in Table 11.2.

We use a paired sampling approach to simultaneously draw returns from both time series. In this case, it is not obvious as to the optimal expected blocksize when sampling in a paired fashion. A simple strategy is to set the paired expected blocksize to be the average of the optimal blocksize for each series. We will give results for a range of blocksizes as a check on the robustness of the bootstrap results. Detailed pseudo-code for block bootstrap resampling is given in Forsyth and Vetzal (2019).

12 Numerical Results

12.1 Stabilization

In some of our initial tests, we observed that the control was not very stable for very large values of the wealth, near the terminal time. We deduced that this was due to the form of the objective function. If $W_t \gg \max(\beta, W^*)$, and $t \to T$, then $Pr[W_T < W^*] \simeq 0$ and $Pr[W_T > \beta] \simeq 1$. In this fortuitous situation for the retiree, the control only weakly effects the objective function. To avoid this problem, when we plotted the heat maps of the optimal controls, we changed the objective function (7.1) to

$$J\left(s,b,t_0^-\right) = \sup_{\mathcal{P}_0 \in \mathcal{A}} \sup_{W^*} \left\{ E_{\mathcal{P}_0}^{X_0^+,t_0^+} \left[W^* + \frac{1}{\alpha} \min(W_T - W^*, 0) + \kappa \mathbf{1}_{W_T > \beta} \overbrace{+\epsilon W_T}^{stabilization} \middle| X(t_0^-) = (s,b) \right] \right\} . \tag{12.1}$$

Equity Weight	$Median[W_T]$	$Mean[W_T]$	5% CVAR
$p = 0.2$	268	359 (0.8)	-357
$p = 0.3$	723	1495 (1.8)	-359
$p = 0.4$	1323	1911 (3.1)	-385
$p = 0.5$	2087	3299 (7.1)	-428
$p = 0.6$	3031	5337 (13)	-489

Table 12.1: *Synthetic market results for constant proportion strategies, assuming the scenario given in Table 11.1. Stock index: real CRSP stocks; bond index: real 30-day T-bills. Parameters from Table 10.1. Real wealth after* 45 *years, measured in thousands of dollars. Statistics based on* 2.56×10^6 *Monte Carlo simulation runs. Numbers in brackets are the standard error at the* 99% *confidence level. The constant proportion strategies have equity fraction* p*.*

We used the value $\epsilon = 10^{-6}$ in the following test cases. Note that using this small value of $\epsilon = 10^{-6}$ gave the same results as $\epsilon = 0$ for the summary statistics, to four digits. This is simply because the states with very large wealth have low probability. However, this stabilization procedure produced more smooth heat maps for large wealth values, without altering the summary statistics appreciably.

12.2 Conservative Investor

We assume that a conservative investor has a portfolio consisting of the CRSP stock index, and a 30-day T-bill index. The extra cost of borrowing is assumed to be $\mu_c^b = .02$ (see equation 2.4). Borrowing is required in the event of portfolio insolvency. We implicitly assume that, in a worst case scenario, the retiree can borrow with the spread $\mu_c^b = .02$, perhaps using residential real estate as collateral. The parameters for the stock and bond processes are fit to the historical data using the threshold method (see Table 10.1). The investment scenario is described in Table 11.1.

Our benchmark strategy is to rebalance to a constant fraction in equities at each rebalancing time $t \in \mathcal{T}$. Table 12.1 shows the summary statistics of Monte Carlo simulations for constant proportion strategies. We assume that the conservative investor wishes to meet (or exceed) the target median as determined for the $p = 0.4$ constant proportion in stocks, as given in Table 12.1. This gives a target median of 1323 (recall that we use thousands as units of wealth, so this actually refers to 1323×10^3). We use $\alpha = .05$ (5% CVAR), and a coarse tolerance in Algorithm 6.1, which gives an estimate of $\kappa = 110$ in equation (7.1). In our grid search we err on the side of selecting κ which generates a median larger than the target.

Table 12.2 shows a convergence test for the solution of the HJB PIDE, for various grid sizes with fixed $\kappa = 110$. We computed and stored the optimal controls for a given grid size, and then used these controls in Monte Carlo simulations. These results indicate that the control on the finest grid is certainly accurate enough for practical purposes. Note that our target Median from the benchmark strategy ($p = 0.4$) was $Median[W_T] = 1323$. The Monte Carlo results indicate that the control actually produced $Median[W_T] = 1340,$ which is slightly larger than the benchmark. Note from Table 12.2 that the 5% CVAR from the optimal strategy is -199, compared with -385 for the benchmark strategy, which is a considerable improvement.

We should mention that we also ran the case with $\kappa = 0$, i.e. our sole objective was to maximize CVAR. The Monte Carlo results using the control computed on the finest grid in Table 12.2 were CVAR $= -190$ and $Median[W_T] = 400$. Compare this with the Monte Carlo results, finest grid, in Table 12.2, which have CVAR $= -199$ and $Median[W_T] = 1340$. This shows that the investor is

	HJB Equation			Monte Carlo		
Grid	$Prob[W_T > 1323]$	CVAR (5%)	W^*	$E[W_T]$	CVAR (5%)	$Median[W_T]$
512×512	0.523	-229	200	1643 (1.6)	-207	1368
1024×1024	0.511	-210	191	1595 (1.6)	-202	1345
2048×2048	0.506	-203	182	1579 (1.6)	-199	1340

TABLE 12.2: *Convergence test, Ambition-CVAR, conservative investor, real stock index: deflated CRSP, real bond index: deflated 30 day T-bills. The target median is* 1323*, which is the median for the constant proportion strategy* $p = 0.4$ *from Table 12.1. Parameters in Table 10.1. The Monte Carlo method used* 2.56×10^6 *simulations. The numbers in brackets are the standard errors at the 99% confidence level.* $\kappa = 110, \alpha = .05$*. Grid refers to the grid used to solve the HJB PDE:* $n_x \times n_b$*, where* n_x *is the number of nodes in the* $\log s$ *direction, and* n_b *is the number of nodes in the* $\log b$ *direction. Units: thousands of dollars (real).*

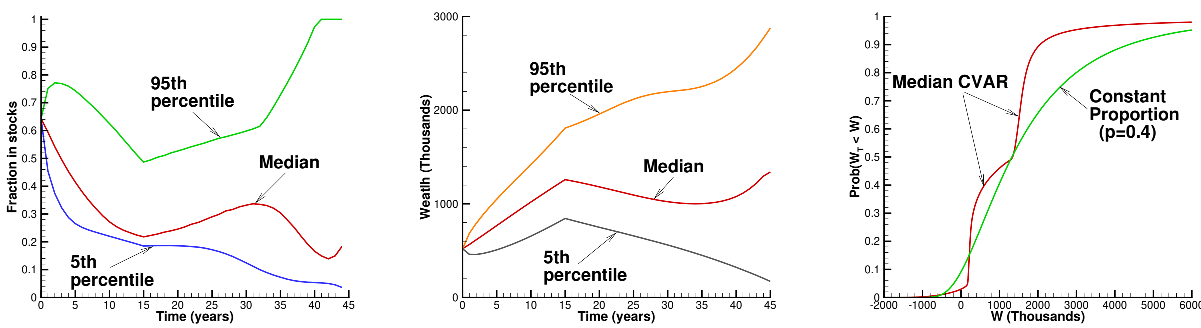

(a) *Percentiles fraction in stocks*

(b) *Percentiles wealth*

(c) *Cumulative distribution function*

FIGURE 12.1: *Scenario in Table 11.1. Optimal control computed from Median-CVAR optimization. Parameters based on the conservative investor, CRSP stocks, 30 day T-bills (see Table 10.1). Finest grid results from Table 12.2. Synthetic market,* 2.56×10^6 *MC simulations.* κ *determined so that* $Median[W_T]$ *is the same as for the* $p = 0.4$ *constant proportion strategy.*

required to give up a large upside in terms of median, in order to obtain a rather small improvement in CVAR.

Figure 12.1 shows the time evolution of the percentiles of the control and the percentiles of portfolio wealth. Note that upon retirement, $t = 15$ years, the median fraction in stocks is less than 0.25, which is certainly a desirable outcome. The median fraction in stocks increases at later times. We will discuss this behaviour when we show the control heat maps. We can also see from Figure 12.1(b) that the fifth percentile of the terminal wealth is positive.

Figure 12.1(c) shows the cumulative distribution functions for the terminal wealth, for both the benchmark strategy and the optimal strategy. Both strategies have approximately the same median, hence both curves intersect at $Prob[W_T < W] = 0.5$. Note that the optimal strategy CDF drops rapidly below the benchmark CDF near $W = 0$.

Another view of the distribution of wealth values is given in Figure 12.2, which shows the probability density function of the internal rate of return (IRR) for the Median-CVAR strategy. The break-even IRR is the rate of return which gives $W_T = 0$. Consistent with the cumulative

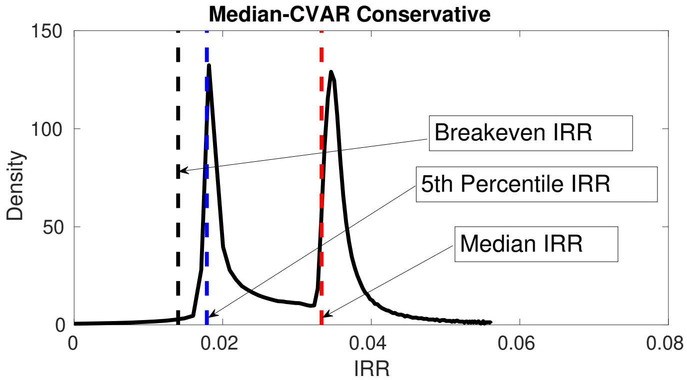

FIGURE 12.2: *Probability density of the Internal Rate of Return (IRR), Median CVAR objective. Parameters based on the conservative investor, CRSP stocks, 30 day T-bills (see Table 10.1).* κ *determined so that* $Median[W_T]$ *is the same as for the* $p = 0.4$ *constant proportion strategy. Maximize* $\{E[(W_T - 183)^-] + \kappa\alpha \; Prob[W_T > 1323]\}$*. Synthetic market,* 2.56×10^6 *MC simulations. Breakeven* $IRR = .014$.

distribution function in Figure 12.1(c), we can see that the IRR density is bimodal, with one peak centered near the breakeven IRR, and another peak centered near the median IRR.

The Median-CVAR optimal control heat map is given in Figure 12.3. Note that the bond heavy control (blue portion of heat map) becomes multiply connected for times greater than 20 years. The lower high bond region is a result of the fact that the control attempts to maximize $E[\min(W_T - W^*, 0)]$, with $W^* \simeq 182$. Once $W_t \gg 182$, and $t > 40$, the strategy switches focus to maximizing $Pr[\mathbf{1}_{W_T > \beta}]$, where $\beta = 1323$. The strategy switches back to bonds again, once $W_t > 1323$. Finally, when $W_t \gg 1323$, the ϵW_T term in equation (12.1) comes into effect, causing the strategy to switch back into stocks. This simply because at this point, $Pr[W_T < 182] \simeq 0$ and $Pr[W_T > 1323] \simeq 1$.

We compute and store the optimal Median-CVAR strategy on the finest grid. We then use this control, but test the strategy in the bootstrapped historical market. Table 12.3 shows the results for various expected blocksizes. While there is some variability in the results for different blocksizes, we can see that the ranking of the strategies is always preserved. The median values for the benchmark strategy and for the Median-CVAR strategy are close for each blocksize, but the 5% CVAR and $Pr[W_T < 0]$ measures are significantly improved for the Median-CVAR policy. Note as well that the probability of ruin, i.e. $Pr[W_T < 0]$ for the Median-CVAR strategy is approximately one third of the ruin probability for the benchmark policy, for each blocksize. These tests indicate that the strategy is robust to model misspecification.

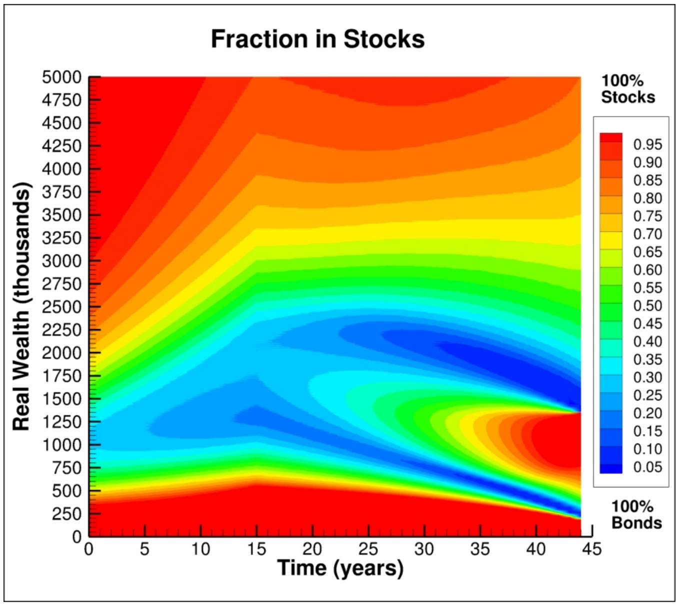

FIGURE 12.3: *Optimal control heat map, Median-CVAR objective. Parameters based on the conservative investor, CRSP stocks, 30 day T-bills (see Table 10.1). κ determined so that $Median[W_T]$ is the same as for the $p = 0.4$ constant proportion strategy. Maximize $\{E[(W_T - 183)^-] + \kappa\alpha\ Prob[W_T > 1323]\}$ (wealth units thousands).*

Strategy	$Median[W_T]$	5% CVAR	Prob$[W_T < 0]$
	$\hat{b} = 1$ year		
$p = 0.4$	1315	-358	0.084
Median-CVAR	1304	-177	0.029
	$\hat{b} = 2$ years		
$p = 0.4$	1324	-334	0.078
Median-CVAR	1323	-96	0.023
	$\hat{b} = 5$ years		
$p = 0.4$	1336	-274	0.068
Median-CVAR	1346	+23	0.014

TABLE 12.3: *Historical market results, conservative strategy, CRSP stock index, 30 day T-bills. W_T denotes real terminal wealth after 45 years, measured in thousands of dollars. Statistics based on 100,000 stationary block bootstrap resamples of the historical data from 1926:1 to 2018:12. $\hat{b}$ is the expected blocksize, measured in years. Estimated optimal blocksize from Table 11.2 is $\hat{b} \simeq 2.0$ years.*

Equity Weight	$Median[W_T]$	$Mean[W_T]$	5% CVAR
$p = 0.3$	1992	2659 (4.2)	-167
$p = 0.4$	2780	3945 (7.0)	-154
$p = 0.5$	3672	5670 (11.7)	-203
$p = 0.6$	4647	7972 (19)	-299
$p = 0.7$	5670	11032 (32)	-423

TABLE 12.4: *Synthetic market results for constant proportion strategies, assuming the scenario given in Table 11.1. Stock index: real CRSP stocks; bond index: real 10 year treasuries. Parameters from Table 10.1. wealth after* 45 *years, measured in thousands of dollars. Statistics based on* 2.56×10^6 *Monte Carlo simulation runs. Numbers in brackets are the standard error at the* 99% *confidence level. The constant proportion strategies have equity fraction* p.

12.3 Aggressive Investor

We assume that an aggressive investor has a portfolio consisting of the CRSP stock index, and the 10 year US treasuries index. The extra cost of borrowing is assumed to be $\mu_c^b = 0.0$ (see equation 2.4), since the average return on a ten year treasury is already higher than the return on a 30-day T-bill. The parameters for the stock and bond processes are fit to the historical data using the threshold method (see Table 10.1). The investment scenario is described in Table 11.1.

Table 12.4 shows the summary statistics of Monte Carlo simulations for constant proportion strategies. We assume that the investor targets the same median return as observed in the synthetic market case with a constant proportion of 0.60 in stocks. The median in this case is 4647 (again, recall that our wealth units are thousands, so this is actually 4647×10^3). We use $\alpha = .05$ (5% CVAR) and a coarse grid search in Algorithm 6.1 gives an estimate of $\kappa = 650$ in equation (7.1). In our grid search we err on the side of selecting κ which generates a median larger than the target.

Table 12.5 shows the convergence tests for the aggressive investor case. The finest grid Monte Carlo simulation has $Median[W_T] = 4714$, 5% CVAR $= -25$, compared with the benchmark $p = 0.6$ strategy in Table 12.4, which gives $Median[W_T] = 4647$, 5% CVAR $= -299$.

We compute and store the controls in the synthetic market, and then carry out bootstrap resampling tests, using these stored controls, in the historical market. Table 12.6 indicates once again that (i) for all blocksizes, the medians of the terminal wealth for the benchmark and Median-CVAR strategy are similar, (ii) the 5% CVAR for the Median-CVAR strategy is consistently significantly larger than for the benchmark strategy, and (iii) the $Prob[W_T < 0]$ for the Median-CVAR strategy is about one-half that of the benchmark solution.

Figure 12.4 shows the percentiles of the fraction in equities and the percentiles of wealth as a function of time, for the bootstrapped historical market. Again we can see the rapid de-risking as retirement ($t = 15$) approaches, followed by a *"risk-on"* behaviour peaking at about 30 years. At retirement, the optimal Median-CVAR strategy has about 30% in equities, compared to the benchmark 60%. Figure 12.4(c) shows the cumulative distribution functions for the Median-CVAR strategy, and for the constant proportion benchmark, in the historical market. This curve is qualitatively similar to the CDFs for the conservative investor case.

Finally, the heat map of controls for the Median-CVAR strategy is plotted in Figure 12.5. Recall that the induced time consistent strategy $TCEQ(\kappa\alpha)$ for this case is the policy which maximizes

$$E\big[\min(W_T - 367, 0)\big] + \kappa\alpha Prob[W_T > 4647] + \epsilon E[W_T] \ . \tag{12.2}$$

Note that we include the stabilization term (see equation (12.1)) to regularize the problem at large

	HJB Equation			Monte Carlo		
Grid	$Prob[W_T > 4647]$	CVAR (5%)	W^*	$E[W_T]$	CVAR (5%)	$Median[W_T]$
512×512	.5132	-38.4	352	5518 (2)	-25.4	4726
1024×1024	.5076	-28.2	364	5514 (2)	-24.8	4716
2048×2048	.5061	-25.6	367	5512 (2)	-24.7	4714

TABLE 12.5: *Convergence test, Ambition-CVAR, aggressive investor, real stock index: deflated CRSP, real bond index: deflated 10 year treasuries. The target median is* 4646.6*, which is the median for the constant proportion strategy* $p = 0.6$ *from Table 12.4. Parameters in Table 10.1. The Monte Carlo method used* 2.56×10^6 *simulations. The numbers in brackets are the standard errors at the 99% confidence level.* $\kappa = 650, \alpha = .05$*. Grid refers to the grid used to solve the HJB PDE:* $n_x \times n_b$*, where* n_x *is the number of nodes in the* $\log S$ *direction, and* n_b *is the number of nodes in the* $\log B$ *direction. Units: thousands of dollars (real).*

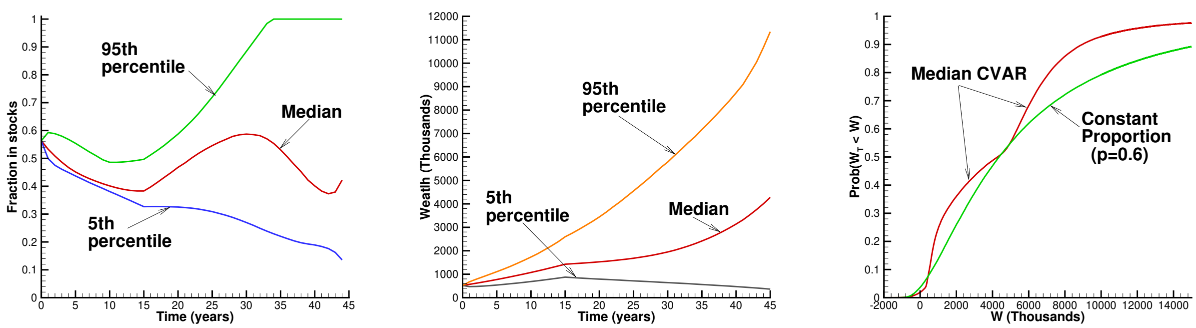

(a) *Percentiles fraction in stocks*

(b) *Percentiles wealth*

(c) *Cumulative distribution function*

FIGURE 12.4: *Scenario in Table 11.1. Optimal control computed from Median-CVAR optimization.* $Median[W_T]$ *is the same as for the* $p = 0.6$ *constant proportion strategy. Parameters based on the aggressive investor, CRSP stocks, 10 year US treasuries (see Table 10.1). Finest grid results from Table 12.2. Stationary block bootstrap of historical data 1926:1-2018:12. Expected blocksize* 0.25 *years.* $Median[W_T]$ *is the same as for the* $p = 0.6$ *constant proportion strategy.*

wealth levels.

We can see that the heat map reflects this objective function as we near $t = T$. For example, consider fixing the time at $t = 40$ years. For very low values of $W_t \ll 367$, the investor has no choice but to invest heavily in stocks, in order to maximize the first term in equation (12.2). If $W_t \simeq 367$, then the investor switches to bonds, in order to preserve the downside risk. As wealth increases ($t = 40$), then the retiree re-risks, now to maximize $Prob[W_T > 4647]$. Once $W_t = 4647$ is reached, the investor de-risks to preserve the gains in the objective function. Finally, when $W_t \gg 4647$, we have that (i) $Prob[W_T > 4647] \simeq 1$ and (ii) $Prob[W_T < 367] \simeq 0$, hence the small term $\epsilon E[W_T]$ comes into play, the investor re-risks once again.

Strategy	$Median[W_T]$	5% CVAR	Prob$[W_T < 0]$
	$\hat{b} = 0.25$ year		
$p = 0.6$	4360	-214	0.037
Median-CVAR	4277	+15	0.019
	$\hat{b} = 0.5$ years		
$p = 0.6$	4462	-250	0.039
Median-CVAR	4436	-18	0.021
	$\hat{b} = 1.0$ years		
$p = 0.6$	4564	-204	0.035
Median-CVAR	4586	+8.0	0.019

TABLE 12.6: *Historical market results, aggressive strategy, CRSP stock index, ten year treasuries. W_T denotes real terminal wealth after 45 years, measured in thousands of dollars. Statistics based on 100,000 stationary block bootstrap resamples of the historical data from 1926:1 to 2018:12. $\hat{b}$ is the expected blocksize, measured in years. Estimated optimal blocksize from Table 11.2 is $\hat{b} \simeq .25$ years.*

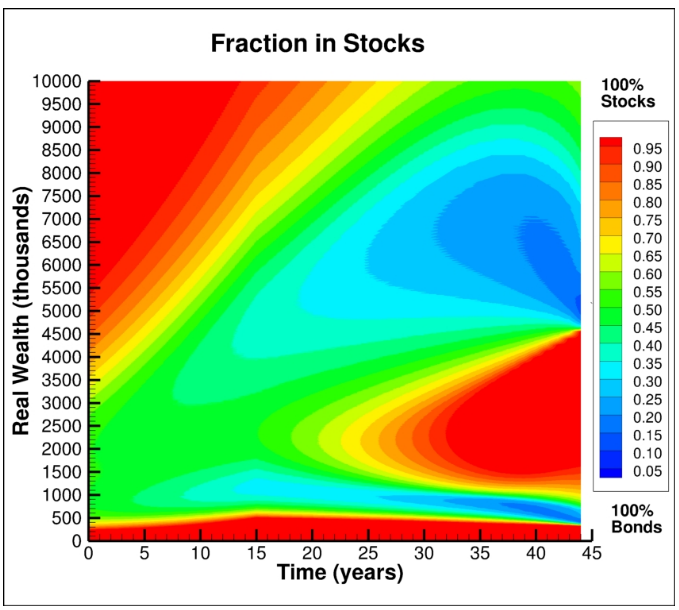

FIGURE 12.5: *Optimal control heat map, Median-CVAR objective. Parameters based on the aggressive investor, CRSP stocks, 10 year US treasuries (see Table 10.1). κ determined so that $Median[W_T]$ is the same as for the $p = 0.6$ constant proportion strategy. Maximize $\{E[(W_T - 367)^-] + \kappa\alpha\ Prob[W_T > 4647]\}$ (wealth units thousands).*

13 Conclusions

Defining Ambition at level β as $Prob[W_T > \beta]$, where W_T is the terminal wealth, we argue that an Ambition-CVAR strategy is appropriate for an investor in the late stages of DC plan accumulation, who is concerned with the risks of portfolio depletion in the decumulation stage. We use a scalarization method to determine points on the Ambition-CVAR frontier.

Suppose we are given a benchmark strategy with $Median[W_T] = \beta$. Then, we can construct the Ambition-CVAR frontier, with Ambition level β. Provided that the Ambition-CVAR frontier has certain properties, we can find the point on the Ambition-CVAR frontier which corresponds to the specified $Median[W_T] = \beta$ from a benchmark strategy (in our examples, a fixed equity proportion). This point is Median-CVAR optimal. Hence, we have found the strategy which has the same median as the benchmark policy, yet maximizes the CVAR (we remind the reader that we have defined CVAR in terms of terminal wealth, not losses, so a larger value is preferred).

The Ambition-CVAR policy (hence also the Median-CVAR control) maximized at time zero is equivalent to an induced time consistent objective function. The induced strategy is (i) identical to the pre-commitment control at the initial time and (ii) the solution of a time consistent problem (under the induced objective function) at all later times. Hence this is an *implementable* strategy, i.e. the investor has no incentive to deviate from the policy computed at time zero at later times.

Our numerical examples show that

- The Median-CVAR optimal control significantly outperforms the benchmark constant proportion strategy, in terms of CVAR as seen at time zero, while preserving the same Median terminal wealth.
- The Median-CVAR control results in a considerable reduction in the probability of ruin, compared to the constant proportion strategy.
- The Median-CVAR median equity allocation at retirement is substantially less than the constant proportion benchmark.
- Bootstrap resampled tests on historical data showed that this ranking of strategies is robust to stochastic process model misspecification.

However, it is clear that the optimal control which minimizes tail risk during decumulation, is complex, as shown in the control heat maps. This illustrates the difficulty of reducing sequence of return risk during decumulation. It is costly, in terms of median return, to reduce tail risk. This suggests that there is a need for a financial product which can mitigate this risk at reasonable cost, while avoiding the use of annuities, which are not popular with retail investors.

Finally, it is possible to incorporate other assets in the portfolio, e.g. trend following or smart beta indices. In the case of more than three underlying assets, the PIDE approach used here will become computationally infeasible. However, a machine learning approach for a high dimensional optimal Median-CVAR control problem would be feasible (Li and Forsyth, 2019).

Acknowledgements

Peter Forsyth acknowledges support from the Natural Sciences and Engineering Research Council of Canada (NSERC), RGPIN-2017-03760.

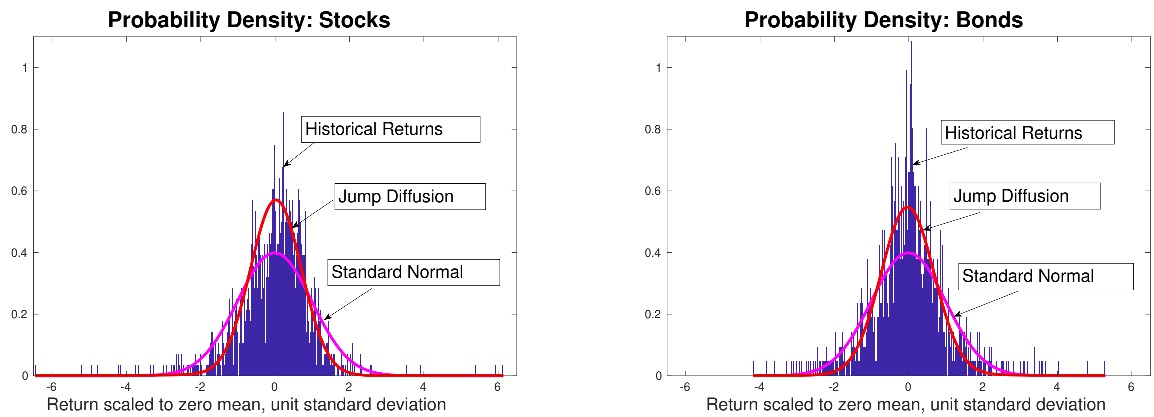

(a) *Log returns and densities, stocks.*

(b) *Log returns and densities, bonds.*

FIGURE A.1: *Actual and fitted log returns for real CRSP value-weighted index, and real 10-year Treasuries. Monthly data, 1926:1-2018:12, scaled to unit standard deviation and zero mean. Standard normal density and fitted double exponential jump diffusion density (threshold, $\theta = 3$) also shown.*

Appendix

A Calibration of Model Parameters

We will follow the common practitioner approach of treating both stock and bond returns as correlated jump diffusion processes, see for example (MacMinn et al., 2014; Lin et al., 2015). In this Appendix, we discuss the estimation of the parameters of the jump diffusion process given by equations (2.1) and (2.3), and equations (2.5) and (2.4).

The data was obtained from the Center for Research in Security Prices (CRSP) on a monthly basis over the 1926:1-2018:12 period.[6] We use the CRSP US equities value weighted index, the one-month T-bill series, and the 10-year US treasury series. All of these various indexes are in nominal terms, so we adjust them for inflation by using the U.S. CPI index, also supplied by CRSP.

Figure A.1(a) shows a histogram of the monthly log returns from the real value-weighted CRSP total return index, scaled to zero mean and unit standard deviation. We superimpose a standard normal density onto this histogram. We also superimpose the fitted density for the double exponential jump diffusion model. The plot shows that the empirical data is leptokurtic, consistent with previous empirical findings for virtually all financial time series. Figure A.1(b) shows the equivalent plot for a constant maturity ten year US treasury index.

A standard technique for parameter estimation is maximum likelihood (ML). However, it is well-known that the use of ML estimation for a jump diffusion model is problematic, due to multiple local maxima and the ill-posedness of trying to distinguish high frequency small jumps from diffusion (Honore, 1998). Consequently, as an alternative to ML estimation, we use the thresholding technique described in Mancini (2009) and Cont and Mancini (2011).

Let $\Delta \hat{X}_i$ be the detrended log return in period i, with period time interval Δt. Suppose we have

[6] More specifically, results presented here were calculated based on data from Historical Indexes, ©2019 Center for Research in Security Prices (CRSP), The University of Chicago Booth School of Business. Wharton Research Data Services was used in preparing this article. This service and the data available thereon constitute valuable intellectual property and trade secrets of WRDS and/or its third-party suppliers.

Data	Stock jumps	Bond jumps	Joint jumps
CRSP, 10-year Treasury	30	36	1
CRSP, 30-day T-bill	30	48	5

TABLE A.1: *Observed jump data, jump diffusion model. Value-weighted CRSP index, 10-year Treasury, 30 day T-bill, deflated by the CPI. Sample period 1926:1 to 2018:12.*

an estimate for the diffusive volatility component $\hat{\sigma}$. Then we detect a jump in period i if

$$\left|\Delta \hat{X}_i\right| > \mathcal{A}\,\hat{\sigma}\,\frac{\sqrt{\Delta t}}{(\Delta t)^{\nu}} \tag{A.1}$$

where $\nu, \mathcal{A} > 0$ are tuning parameters (Shimizu, 2013), and $\hat{\sigma}$ is our most recent estimate of volatility. An iterative method is used to determine the parameters (Clewlow and Strickland, 2000). The intuition behind equation (A.1) is simple. If we choose $\mathcal{A} = 3$, say, and $\nu \ll 1$, then equation (A.1) identifies an observation as a jump if the observed log return exceeds a 3 standard deviation geometric Brownian motion change. Typically, ν in equation (A.1) is quite small, $\nu \simeq .01 - .02$. For details, we refer the reader to Dang and Forsyth (2016). As described in Dang and Forsyth (2016), we replace $\mathcal{A}/(\Delta t)^{\nu}$ by the parameter θ. Use of $\theta = 3$ for monthly data results in fairly infrequent, large jumps. Additional details concerning the threshold estimators can be found in Dang and Forsyth (2016) and Forsyth and Vetzal (2017).

As noted in Remark 2.1, we have assumed that stock and bond jumps are independent. As a point of information, in Table A.1 we show some relevant statistics for the CRSP stock index and the 10-year Treasury series, as well as the CRSP index and the 30-day T-bill series, based on the threshold filtering technique for estimation of jumps. In the CRSP-10 year series, there is only one joint stock-bond jump out of 65 unique jump events. For the CRSP-30 day series, there are 5 joint stock-bond events, out of 73 unique jump events. This justifies (to a certain extent) the assumption that the stock-bond jumps are independent.

References

Basu, A. K., A. Byrne, and M. E. Drew (2011). Dynamic lifecycle strategies for target date retirement funds. *Journal of Portfolio Management 37*(2), 83–96.

Bengen, W. (1994). Determining withdrawal rates using historical data. *Journal of Financial Planning 7*, 171–180.

Bernhardt, T. and C. Donnelly (2018). Pension decumulation strategies: A state of the art report. Technical Report, Risk Insight Lab, Heriot Watt University.

Blake, D., D. Wright, and Y. Zhang (2014). Age-dependent investing: Optimal funding and investment strategies in defined contribution pension plans when members are rational life cycle financial planners. *Journal of Economic Dynamics and Control 38*, 105–124.

Braughtigam, M., M. Guillen, and J. P. Nielsen (2017). Facing up to longevity with old actuarial methods: A comparison of pooled funds and income tontines. *The Geneva Papers on Risk and Insurance: Issues and Practice 42*, 406–422.

Campanele, C., C. Fugazza, and F. Gomes (2015). Life-cycle portfolio choice with liquid and illiquid financial assets. *Journal of Monetary Economics 71*, 67–83.

Clewlow, L. and C. Strickland (2000). *Energy Derivatives: Pricing and Risk Management.* London: Lacima Group.

Clift, S. S. and P. A. Forsyth (2008). Numerical solution of two asset jump diffusion models for option valuation. *Applied Numerical Mathematics 58*, 743–782.

Cocco, J. F., F. J. Gomes, and P. J. Maenhout (2005). Consumption and portfolio choice over the life cycle. *Review of Financial Studies 18*, 491–533.

Cont, R. and C. Mancini (2011). Nonparametric tests for pathwise properties of semimartingales. *Bernoulli 17*, 781–813.

Dang, D.-M. and P. A. Forsyth (2016). Better than pre-commitment mean-variance portfolio allocation strategies: a semi-self-financing Hamilton-Jacobi-Bellman equation approach. *European Journal of Operational Research 250*, 827–841.

Dang, D.-M., P. A. Forsyth, and Y. Li (2016). Convergence of the embedded mean-variance optimal points with discrete sampling. *Numerische Mathematik 132*, 272–302.

Dichtl, H., W. Drobetz, and M. Wambach (2016). Testing rebalancing strategies for stock-bond portfolos across different asset allocations. *Applied Economics 48*, 772–788.

Esch, D. N. and R. O. Michaud (2014). The false promise of target date funds. Working paper, New Frontier Advisors, LLC.

Fagereng, A., C. Gottlieb, and L. Guiso (2017). Asset market participation and portfolio choice over the life-cycle. *Journal of Finance 72*, 705–750.

Feng, R. and B. Yi (2019). Quantitative modeling of risk management strategies: Stochastic reserving and hedging of variable annuity guaranteed benefits. *Insurance: Mathematics and Economics 85(c)*, 60–73.

Forsyth, P. and G. Labahn (2019). $\epsilon-$Monotone Fourier methods for optimal stochastic control in finance. *Journal of Computational Finance 22:4*, 25–71.

Forsyth, P. A. (2020). Multi-period mean CVAR asset allocation: Is it advantageous to be time consistent? *SIAM Journal on Financial Mathematics 11:2*, 358–384.

Forsyth, P. A. and K. R. Vetzal (2014). An optimal stochastic control framework for determining the cost of hedging of variable annuities. *Journal of Economic Dynamics and Control 44*, 29–53.

Forsyth, P. A. and K. R. Vetzal (2017). Dynamic mean variance asset allocation: Tests for robustness. *International Journal of Financial Engineering 4*, 1750021:1–1750021:37. DOI: 10.1142/S2424786317500219.

Forsyth, P. A. and K. R. Vetzal (2019). Optimal asset allocation for retirement savings: deterministic vs. time consistent adaptive strategies. *Applied Mathematical Finance 26:1*, 1–37.

Forsyth, P. A., K. R. Vetzal, and G. Westmacott (2019). Management of portfolio depletion risk through optimal life cycle asset allocation. *North American Actuarial Journal 23:3*, 447–468.

Forsyth, P. A., K. R. Vetzal, and G. Westmacott (2020). Asset allocation for DC pension decumulation with a variable spending rule. To appear, ASTIN Bulletin.

Graf, S. (2017). Life-cycle funds: Much ado about nothing? *European Journal of Finance 23*, 974–998.

Honore, P. (1998). Pitfalls in estimating jump diffusion models. Working paper, Center for Analytical Finance, University of Aarhus.

Horneff, V., R. Maurer, O. S. Mitchell, and R. Rogalla (2015). Optimal life cycle portfolio choice with variable annuities offering liquidity and investment downside protection. *Insurance: Mathematics and Economics 63*, 91–107.

Kitces, M. E. and W. D. Pfau (2015). Retirement risk, rising equity glide paths, and valuation-based asset allocation. *Journal of Financial Planning 28:3*, 38–48.

Kou, S. G. (2002). A jump-diffusion model for option pricing. *Management Science 48*, 1086–1101.

Kou, S. G. and H. Wang (2004). Option pricing under a double exponential jump diffusion model. *Management Science 50*, 1178–1192.

Li, Y. and P. A. Forsyth (2019). A data driven neural network approach to optimal asset allocation for target based defined contribution pension plans. *Insurance: Mathematics and Economics 86*, 189–204.

Lin, Y., R. MacMinn, and R. Tian (2015). De-risking defined benefit plans. *Insurance: Mathematics and Economics 63*, 52–65.

Ma, K. and P. A. Forsyth (2016). Numerical solution of the Hamilton-Jacobi-Bellman formulation for continuous time mean variance asset allocation under stochastic volatility. *Journal of Computational Finance 20*(1), 1–37.

MacDonald, B.-J., B. Jones, R. J. Morrison, R. L. Brown, and M. Hardy (2013). Research and reality: A literature review on drawing down retirement financial savings. *North American Actuarial Journal 17*, 181–215.

MacMinn, R., P. Brockett, J. Wang, Y. Lin, and R. Tian (2014). The securitization of longevity risk and its implications for retirement security. In O. S. Mitchell, R. Maurer, and P. B. Hammond (Eds.), *Recreating Sustainable Retirement*, pp. 134–160. Oxford: Oxford University Press.

Mancini, C. (2009). Non-parametric threshold estimation models with stochastic diffusion coefficient and jumps. *Scandinavian Journal of Statistics 36*, 270–296.

Michaelides, A. and Y. Zhang (2017). Stock market mean reversion and portfolio choice over the life cycle. *Journal of Financial and Quantitative Analysis 52*, 1183–1209.

Milevsky, M. A. and T. S. Salisbury (2015). Optimal retirement income tontines. *Insurance: Mathematics and Economics 64*, 91–105.

Patton, A., D. Politis, and H. White (2009). Correction to: automatic block-length selection for the dependent bootstrap. *Econometric Reviews 28*, 372–375.

Peijnenburg, K., T. Nijman, and B. J. Werker (2016). The annuity puzzle remains a puzzle. *Journal of Economic Dynamics and Control 70*, 18–35.

Piscopo, G. and S. Haberman (2011). The valuation of guaranteed lifelong withdrawal benefit options in variable annuity contracts and the impact of mortality risk. *North American Actuarial Journal 15(1)*, 59–76.

Politis, D. and J. Romano (1994). The stationary bootstrap. *Journal of the American Statistical Association 89*, 1303–1313.

Politis, D. and H. White (2004). Automatic block-length selection for the dependent bootstrap. *Econometric Reviews 23*, 53–70.

Poterba, J. M., J. Rauh, S. F. Venti, and D. A. Wise (2009). Life-cycle asset allocation strategies and the distribution of 401(k) retirement wealth. In D. A. Wise (Ed.), *Developments in the Economics of Aging*, pp. 15–50. Chicago: University of Chicago Press.

Rockafellar, R. T. and S. Uryasev (2000). Optimization of conditional value-at-risk. *Journal of Risk 2*, 21–42.

Rupert, P. and G. Zanella (2015). Revisiting wage, earnings, and hours profiles. *Journal of Monetary Economics 72*, 114–130.

Shimizu, Y. (2013). Threshold estimation for stochastic differential equations with jumps. *Proceedings of the 59th ISI World Statistics Conference*, Hong Kong.

Staden, P. V., D.-M. Dang, and P. Forsyth (2018). Time-consistent mean-variance portfolio optimization: a numerical impulse control approach. *Insurance: Mathematics and Economics 83*, 9–28.

Strub, M., D. Li, and X. Cui (2019). An enhanced mean-variance framework for robo-advising applications. SSRN 3302111.

Tankov, P. and R. Cont (2009). *Financial Modelling with Jump Processes*. New York: Chapman and Hall/CRC.

Vigna, E. (2014). On efficiency of mean-variance based portfolio selection in defined contribution pension schemes. *Quantitative Finance 14*, 237–258.

Waring, M. B. and L. B. Siegel (2015). The only spending rule article you will ever need. *Financial Analysts Journal 71*(1), 91–107.

Westmacott, G. and S. Daley (2015). The design and depletion of retirement portfolios. PWL Capital White Paper.

Xu, B. (2018). Option pricing under shared-jump diffusion model by Fourier space time-stepping method. MMath Essay, University of Waterloo.